Submarine eruption-fed and resedimented pumice-rich facies: the Dogashima Formation (Izu Peninsula, Japan)

Martin Jutzeler[1*], Jocelyn McPhie[1], Sharon R. Allen[1]

1: CODES – ARC Centre of Excellence in Ore Deposits, University of Tasmania, PO Box 79, Hobart 7005, Australia

First author's current contact address:

Dr. Martin Jutzeler

National Oceanography Centre, Southampton

European Way, Waterfront Campus

Southampton, SO14 3ZH

United Kingdom

jutzeler@gmail.com

+44 23 80596 559

Keywords: submarine pumice; high-concentration density current; hydraulic sorting; eruption-fed; resedimented; Dogashima Formation

Abstract

In the Izu Peninsula (Japan), the Pliocene pumice-rich Dogashima Formation (4.55 Ma +/- 0.87 Ma) displays exceptional preservation of volcaniclastic facies that were erupted and deposited in a below wave-base marine setting. It includes high-concentration density current deposits that contain clasts that were emplaced hot, indicating an eruption-fed origin. The lower part of the Dogashima 2 unit consists of a very thick sequence (<12 m) of massive grey andesite breccia restricted to the base of a submarine channel, gradationally overlain by pumice breccia, which is widespread but much thinner and finer in the overbank setting. These two breccias share similar mineralogy and crystal composition, and are considered to be co-magmatic, and derived from the destruction of a submarine dome by an explosive, pumice-forming eruption. The two breccias were deposited from a single, explosive eruption-fed, sustained, sea-floor-hugging, water-supported, high-concentration density current in which the clasts were sorted according to their density. At the rim of the channel, localised good hydraulic sorting of clasts and stratification in the pumice breccia are interpreted to reflect local current expansion and unsteadiness rather than to be the result of hydraulic sorting of clasts during fall from a submarine eruption column and/or umbrella plume. A bimodal coarse (>1 m) pumice- and ash-rich bed overlying the breccias may be derived from delayed settling of pyroclasts from suspension. In Dogashima 1 and 2, thick cross- and planar-bedded facies composed of sub-rounded pumice clasts are intercalated with eruption-fed facies, implying inter-eruptive erosion on the flank of a submarine volcano, and below wave-base resedimentation.

Introduction

The explosive nature of submarine volcanic activity is clearly evident from uplifted successions (e.g. Fiske and Matsuda 1964; Fiske 1969; Cas and Wright 1991; McPhie et al. 1993; Kano et al. 1994, 1996; Kano 1996, 2003; Allen and McPhie 2000, 2009; Raos and McPhie 2003; White et al. 2003; Stewart and McPhie 2004) and historical eruptions (Reynolds et al. 1980; Fiske et al. 1998; Kano 2003; Rivera et al. 2013; Jutzeler et al. 2014), and can be inferred from the presence of modern calderas on the sea-floor (Wright and Gamble 1999; Fiske et al. 2001; Tani et al. 2008; Carey et al. 2014). A wide spectrum of pyroclastic facies has been reported in submarine successions (e.g. Wright 1996; Wright and Gamble 1999). An emerging problem is related to distinguishing eruption-fed submarine pyroclastic facies from those produced by resedimentation and reworking processes (Cas et al. 1990; Cas and Wright 1991; McPhie et al. 1993; Allen and McPhie 2000, 2009; White 2000; Schneider et al. 2001; Kano 2003; White et al. 2003; Allen and Freundt 2006; Jutzeler 2012; Jutzeler et al. 2014). For eruptions that have not been witnessed, a careful facies analysis of the deposits, together with clast vesicularity and compositional data, offer a means of reconstructing the eruptive activity and making the eruption-fed versus resedimented distinction. In particular, submarine explosive eruption-fed facies are thought to be characterised by thick to extremely thick, laterally extensive beds composed mainly of angular pyroclasts; the beds may be massive or show weak normal (dense clasts) or reverse (vesicular clasts) grading (McPhie et al. 1993).

The Dogashima Formation on the Izu Peninsula, Japan, was part of the open-marine, rear-Izu-Bonin arc (Tani et al. 2011) during the Pliocene (Fiske 1969; Cashman and Fiske 1991; Tamura et al. 1991; Tamura 1994). Palæo-temperature measurements on dense clasts in an iconic unit of massive grey andesite breccia in the Dogashima Formation (Tamura et al.

1991), hereafter named D2-2, indicate that these clasts were hot at deposition. This unit grades into white pumice breccia (D2-3), implying synchronous deposition of both units and an eruption-fed origin. Therefore, the facies characteristics exposed at Dogashima provide a guide to infer the critical distinction between explosive eruption-fed and resedimented pumice-rich facies.

High-intensity subaqueous explosive eruptions that produce abundant low-density pumice clasts ("neptunian eruptions"; Allen and McPhie 2009) involve eruption columns that are prone to collapse as a result of the rapid increase in density of single pumice clasts and of the eruption column as the gas (magmatic steam) cools and condenses as a result of mixing with sea water (Kato 1987; Kano 1996; Kano et al. 1996; Allen et al. 2008). The pumice lapilli are then transported away from the vent in cold or lukewarm, water-supported, sea-floor hugging density currents (e.g. Allen et al. 2008; Allen and McPhie 2009). In some cases, temperature and textural data demonstrated that part of the clasts were hot during transport and deposition (Tamura et al. 1991; Kano et al. 1994). In some cases, eruptions may be sufficiently powerful that some of the erupted pyroclasts reach the water surface before being sufficiently waterlogged to sink, creating pumice rafts, such as during the July 2012 Havre eruption (Carey et al. 2014; Jutzeler et al. 2014). Subaqueous pumice-rich eruption columns may produce neutrally buoyant, laterally spreading suspensions of pyroclasts, but these suspensions are composed almost exclusively of pyroclasts with slow settling velocities, such as fine (<2 mm) glass shards, crystals and insufficiently waterlogged, coarse pumice clasts (Kano 2003; Allen and McPhie 2009). Clast rounding may not significantly change during transport in pumice-rich density currents in below wave-base environments, as clast impacts are buffered by water (White 2000), and saturated pumice clasts have specific gravities only slightly above that of water (e.g. Manville et al. 1998, 2002) and are therefore easily mobilised.

The Dogashima Formation exposes outstanding outcrops allowing detailed reconstruction of the eruption sequence from facies analysis. The Dogashima Formation was generated by a combination of pumice-forming explosive eruptions, lava dome growth and destruction, and inter-eruptive sedimentation. In particular, this study examines the relationship between lava clasts issued from the destruction of a hot lava dome, and pumice clasts formed by a submarine explosive eruption that destroyed the lava dome.

The Dogashima Formation is also very important because it was deposited in a submarine channel and its overbank, which are well exposed in cross-section. In such island arc settings, the submarine flanks of volcanoes are incised by channels and canyons that focus the downslope movement of sediment and water (e.g. Cas et al. 1990; Gardner 2010; Watt et al. 2012). Complex, channelled sea-floor bathymetry and large-scale dune fields are clearly observed around the submerged portions of modern volcanic arcs in swath bathymetry and submarine camera data (e.g. Wright 2001; Gardner 2010). However, access to these modern settings is limited and cross-sections are rarely exposed. Detailed lithofacies information on the volcaniclastic facies that form in and around submarine channels are best obtained from well exposed and accessible uplifted successions. In the Dogashima Formation, the channel is filled by pumice-rich pyroclastic deposits emplaced by eruption-fed, sea-floor hugging, high-concentration density currents, and overlain by cross- and planar bedded, pumice-rich facies interpreted to result from reworking and resedimentation by high-energy tractional currents in a below wave-base environment.

We present new high-resolution stratigraphic, geochemical, U-Pb ages from zircons, componentry and grain size data for the Dogashima Formation. We use facies characteristics to reconstruct the eruption style and sequence, and explore the sedimentation processes operating in the submarine channel in response to the voluminous influx of pyroclasts.

Terminology

The term breccia is non-genetic and used for a clastic aggregate composed mostly of angular clasts >2 mm (Fisher 1961). Matrix is used for components <2 mm. Fine breccia is used hereafter for breccia with an average clast size <10 cm. Fine grained facies are referred to as pumice sandstone (1/16–2 mm) and shard-rich siltstone (1/256–1/16 mm) without implying genesis. Non- to poorly vesicular (<20 vol.% vesicles) clasts are termed dense clasts. Bed thickness terms follow Ingram (1954); the term "extremely thick" refers to beds >10 m thick. Volume percentages of clasts and grain size distributions of the volcaniclastic facies were calculated by image analysis and functional stereology (Jutzeler et al. 2012). Geochemical and geochronological analyses were carried out at the University of Tasmania (Australia); clast compositions were determined by X-ray fluorescence (XRF) with a Philips PW1480, whereas crystal analyses were performed on a Cameca 100X electron microprobe; the age of the formation was calculated from U-Pb in zircons by LA-ICP-MS.

Geological setting of the Dogashima Formation

The Dogashima Formation is part of the Miocene-early Pliocene volcanogenic Shirahama Group that covers 500 km^2 on the Izu Peninsula, Honshu, Japan (Ibaraki 1981; Tamura 1994; Geological Survey of Japan 2010; Tani et al. 2011). The Shirahama Group is part of the northern extension of the Izu-Bonin arc, which is related to the westward subduction of the northwestern margin of the Pacific plate under the Philippine plate (Taylor 1992; Tani et al. 2011). Northwestern subduction of the Philippine plate beneath the Eurasian plate (including Japan) resulted in collision and uplift of the northern segment of the Izu-Bonin arc (including the Shirahama Group) at ~1 Ma (Huchon and Kitazato 1984).

The Shirahama Group spans 5.5–1.7 Ma (U-Pb in zircons; Tani et al. 2011) and comprises diverse volcanic and subvolcanic facies (lavas, dykes, cryptodomes and volcaniclastic facies). The succession is little deformed and virtually unaltered. Most lavas and intrusions range in composition from basaltic andesite to dacite; basalt and rhyolite are rare (Tamura 1994). This group is thought to include the products of at least six scattered and overlapping eruption centres (Sawamura et al. 1970; Kano 1983, 1989; Yamada and Sakaguchi 1987).

Although the environments of eruption and deposition of the Shirahama Group are poorly constrained, the widespread presence of numerous planktonic foraminifera species (e.g. Ibaraki 1981) suggests that an open-marine environment predominated. The abundance of hyaloclastite and pillow lavas throughout the Shirahama Group and in particular in the Matsuzaki Formation (Kano 1983, 1989; Tamura 1990, 1994) also attests to a submarine environment. An undated island may have been present near Shimoda and Shirahama towns, <20 km southeast of the present Dogashima, because conglomerate occurs in the late Miocene Asahi Formation, and the early Pliocene Harada Formation includes cross-bedded, coastal channel facies, calcarenite and limestone (Matsumoto et al. 1985). Gordee et al. (2008) reported undated conglomerate beds that contain charcoal fragments and shells 11 km south of Dogashima, reflecting input from a subaerial island. From rare earth element abundances and mineral assemblages in lavas, Tani et al. (2011) proposed a rear-arc setting for the Shirahama Group, >20 km from the Izu-Bonin volcanic front. This distance from the arc is consistent with the Shirahama Group having accumulated in an open-marine setting. The paucity of subaerially sourced components in formations above and below the Dogashima Formation is also consistent with an open-marine, below wave-base environment that included mostly underwater volcanoes.

The Dogashima Formation

The Dogashima Formation is exposed over 1.5 km^2 and is 5 to >80 m thick, suggesting a volume of at least ~10^7 m^3 (Fig. 1). It includes four main subdivisions (Fiske 1969; Tamura 1990, 1994), here named Kamegoiwa, and Dogashima 1, 2 and 3 up stratigraphy (Fig. 2). The formation is dominated by white pumice clasts (overall 80 vol.%) and crystals fragments. The succession is little deformed and virtually unaltered; numerous joints and faults have a constant northerly strike over the whole area, and overall show little or no displacement. The stratigraphy of the Dogashima Formation was logged at twelve localities, mostly along the coast. The beds in the Dogashima Formation from localities A-F have a ~5 m vertical offset above the beds of localities G-J, suggesting a sub-vertical fault south of locality G (Fig. 1). Beds in the Dogashima Formation are tilted ~10° northeastwards. The mapped area (Fig. 1) is delimited by subvertical faults and intrusions to the north, and by the Matsuzaki Formation to the south (Tamura 1994). The Matsuzaki Formation comprises coherent andesite, monomictic andesite breccia and mafic scoria lapilli. Some clasts derived from the Matsuzaki Formation are present in the Dogashima Formation. The Dogashima Formation is intercalated with the Matsuzaki Formation, and is distinguished from it by the presence of tabular, pumice-rich units.

Components of the Dogashima Formation

The Dogashima Formation contains numerous, mainly andesitic clast types that differ in colour, vesicularity, mineralogy and composition (Fig. 3; Table 1). Dogashima 1 and Dogashima 2 are dominated by white andesitic pumice lapilli (Fig. 4; Table 1), whereas the underlying Kamegoiwa pumice breccia is dominated by aphyric rhyolitic pumice clasts; Dogashima 3 is dominated by andesite breccia. Many of the coarsest white andesitic pumice clasts (>30 cm) have remnants of quenched margins. Grey andesite clasts are dense; mostly coarse (10-50 cm) and equant, and a few outsized clasts (up to 10 m) occur in groups.

Numerous grey andesite clasts are ovoid, have quenched margins and radial joints (Fig. 3 a,b,c); rare (<0.1 vol.%) clasts are fluidal (Table 1). In unit D2-2 near the base of Dogashima 2, the thermoremanent temperatures of very coarse, ovoid grey andesite clasts indicate deposition at 450°C (Tamura et al. 1991). Plagioclase-phyric andesitic inclusions within the grey andesite clasts are tholeiitic and follow the compositional trend of the Dogashima Formation although they differ petrographically (Fig. 4). Red andesite clasts can be differentiated from the grey andesite clasts only by the colour of their groundmass; both are dense and plagioclase-pyroxene-phyric (15-20 vol.% phenocrysts), although the red andesite has slightly higher FeO and lower K_2O compared with the grey andesite (Online Resource 1). The matrix in units of the Dogashima Formation is typically composed of crystals fragments (plagioclase, pyroxene) and other particles of identical aspect and composition to the clasts (Table 1); fine (<1/16 mm) components are mostly minor (<5 vol.%).

The bulk clast and feldspar compositions of the Dogashima Formation (Fig. 4a,b; Online Resources 1, 2) match the compositional range of the Shirahama Group (Tamura 1995), and are transitional between its tholeiitic and calc-alkaline series. The white pumice clasts of Dogashima 1 are very similar in mineralogy and composition to those of Dogashima 2, whereas the grey andesite clasts are slightly less evolved than the white pumice clasts (Fig. 4). Rarely, elongate blebs of grey andesite occur within white pumice (Fig. 3e). These similarities strongly suggest that the white pumice, grey andesite and red andesite were co-magmatic. In addition, microprobe analyses of plagioclase phenocrysts in white pumice clasts and grey andesite clasts, plagioclase crystal fragments, and plagioclase microlites in the grey andesite clasts from Dogashima 2 are similar and define a single trend (Fig. 4c; Online Resource 2). Overall, the pumice clasts have a higher loss on ignition (LOI; 6-12.5 wt.%; Online Resource 1) compared with dense clasts (LOI ≤3 wt.%), and are also higher in the mobile major elements K_2O and Na_2O. Zircons in the white pumice clasts and grey andesite

clasts in Dogashima 1 and 2 give an age of 4.55±0.87 Ma (U-Pb analysed by LA-ICP-MS; Online Resource 3), consistent with the age of other nearby formations in the Shirahama Group (Tani et al. 2011).

Hydrothermally altered volcanic clasts are a minor but ubiquitous component in the Dogashima Formation, and are up to >2 m in diameter. Many units in Dogashima 1 and 2 include clasts identical to those present in the underlying successions, such as white aphyric pumice from the Kamegoiwa pumice breccia and dark andesite clasts from the Matsuzaki Formation. The dark andesite clasts of the Matsuzaki Formation and the coarsely porphyritic andesite clasts in Dogashima 3 are similar in composition to the grey andesite clasts of Dogashima 2 (Fig. 4). White aphyric pumice clasts are angular tube pumice up to 40 cm diameter. The grey scoria clasts and white aphyric pumice clasts are distinct from the compositional field of the other clasts of the Dogashima Formation, although they fall within the overall trend of the Shirahama Group (Fig. 4). The coarsely porphyritic andesite clasts in Dogashima 3 contain more phenocrysts and have a coarser groundmass than the grey andesite clasts in Dogashima 2. No palæo-temperature data are available for the coarsely porphyritic andesite clasts.

Kamegoiwa pumice breccia

The Kamegoiwa pumice breccia is up to 10 m thick and exposed over few outcrops in the southern part of the studied area (Locality K, Figs 1, 5, 6). It is intercalated within the Matsuzaki Formation, overlying brown scoria beds and underlying lavas. The Kamegoiwa pumice breccia consists of two internally stratified pumice breccia beds composed of white aphyric pumice clasts. At the base, there is a high concentration of brown scoria clasts derived from the Matsuzaki Formation (Fig. 7). The matrix is chiefly composed of crystal

fragments; grey banded pumice and hydrothermally altered volcanic clasts are common. Although bed contacts are hidden by sea level, lavas/intrusions of the Matsuzaki Formation, and faults, the presence of white aphyric pumice clasts from the Kamegoiwa pumice breccia in Dogashima 1 and 2 indicates it was unlithified and exposed on the sea floor at the time of deposition of Dogashima 1 and 2.

Dogashima 1

The pumice-rich Dogashima 1 is >15 m thick, mostly exposed in the southern part of the studied area, and overlies the Matsuzaki Formation at locality A with an erosional contact (Figs 1, 2, 5, 6; Table 2). Dogashima 1 is composed of multiple, laterally extensive or lenticular, thick graded beds of pumice breccia (Fig. 8a,b), thin to very thick cross-bedded, planar-bedded and normally graded pumice breccia/sandstone (Fig. 8c,d), medium to very thick beds of polymictic volcanic breccia (Fig. 8b,e,f) and thin to medium beds of shard-rich siltstone (Table 2). From localities A to E, the bases of two polymictic volcanic breccia beds in Dogashima 1 are sharp, discordant surfaces that truncate the underlying beds, indicating erosion, in particular at localities A and B (Figs 2a,b, 8b,e).

Dogashima 2

Dogashima 2 is 15 to 30 m thick, covers the whole area, and is composed of eight stratigraphic units (Figs 5, 6; Table 2). It is dominated by white pumice clasts (chiefly 60–95 vol.%). The most prominent units are the grey andesite breccia (D2-2) and the overlying pumice breccia (D2-3) that are separated by a gradational to sharp contact (Fig. 2c, 3a, 9a). The basal contact of Dogashima 2 is a 600-m-wide, 15-m-deep disconformity carved into beds of Dogashima 1. At locality A (Fig. 2a), Dogashima 2 directly overlies a disconformable

267 contact on coherent andesite and monomictic andesite breccia of the Matsuzaki Formation.
268 Palæo-lows (>50 m wide) are visible at localities G-east and G-west (Fig. 9), and between
269 localities A and B. The disconformity is less pronounced in the northern localities H and I
270 where Dogashima 2 overlies the stratified pumiceous facies of Dogashima 1.

271 The main basal unit (D2-2) is very thick (up to 7 m) massive grey andesite breccia (D2-2)
272 that occurs over the southern and central part of the study area between localities A to G-east
273 (Figs 3a, 5, 9a; Table 1). Unit D2-2 has a sharp, discordant contact with Dogashima 1, and is
274 dominated (up to 90 vol.%) by coarse, grey andesite clasts, some of them with quenched
275 margins and rare fluidal shapes. Very coarse (1-10 m) grey andesite clasts occur in clusters
276 that show overall coarse-tail reverse grading. At locality A, D2-2 overlies polymictic volcanic
277 breccia (D2-1) that contains dark andesite clasts of the Matsuzaki Formation (Fig. 2a). Here,
278 D2-2 also contains conspicuous hydrothermally altered volcanic clasts as well as grey
279 andesite clasts, and is finer grained (average 16 cm) than at the other localities (average 25-50
280 cm). The presence of chilled margins on grey andesitic clasts in massive grey andesite
281 breccia in the middle of the formation (unit D2-2 in this paper; Fig. 3) and thermoremanent
282 temperatures of 450°C in clast rims (at 5 cm depth in the clast) at deposition led Tamura et al.
283 (1991) to interpret this unit as the deposit of a “hot pyroclastic debris flow”.

284 D2-2 is overlain by a 6-to 10-m-thick pumice breccia unit (D2-3) with a sharp to gradational
285 lower contact, depending on the locality (Table 2; Figs 2c, 3c, 5, 9a). The pumice breccia is
286 exposed over the central and northern parts of the study area, between localities C and I; its
287 original distribution to the south (localities A, B) is unknown as D2-2 is the uppermost
288 preserved layer (Fig. 2a). D2-3 mostly consists of white pumice clasts (>20-30 vol.%) in a
289 matrix of finer (<2 mm) pumice and plagioclase and pyroxene crystal fragments; sub-ordinate
290 grey andesite clasts and minor hydrothermally altered volcanic clasts occur throughout
291 (Tables 1, 2). D2-3 exhibits very strong lateral facies variations. It is massive to normally

graded in its southernmost exposures (localities C to F), stratified and reversely graded at locality G-east, and internally stratified and finer grained in the northern part of the studied area (localities G-west, H and I; Figs 6, 9b,c). The upper part of the pumice breccia (beds D2-3d and D2-3-e) at locality G-east is reversely graded, and shows strong bimodality in the size of pumice (coarse) and dense (fine) clasts, reflecting a hydraulically well-sorted deposit (Fig. 10c,d). In general, D2-3 overlies D2-2, however at locality G-east, a 1-m-thick, ~5-m-long lens of pumice breccia with similar texture and composition to D2-3 occurs below D2-2 (Fig. 11). At G-east, D2-3 is overlain with a gradational contact by medium to thick beds of planar stratified pumice breccia (D2-4; Fig. 9a,c) and by a very thick, diffusely stratified, fine pumice breccia (D2-5; Fig. 9a,b) in sharp contact with D2-4.

Localities G-west to I provide the most complete exposure of the upper part of Dogashima 2, which comprises tabular to lenticular, cross-bedded pumice breccia-conglomerate (D2-6), planar bedded pumice breccia (D2-7) and cross-bedded pumice breccia-conglomerate (D2-8) at the top (Table 2; Figs 5, 6, 9b, 12). At locality H and I, exceptional bimodality in the size of pumice clasts characterises the planar bedded pumice breccia (D2-7); very coarse pumice clasts (up to 1 m) occur in a diffusely stratified matrix chiefly composed of white pumice clasts (mostly <2 mm). At localities C, I and J, Dogashima 2 is separated from the weakly stratified andesite breccia of Dogashima 3 by a sharp erosional contact (Figs 2c, 5).

Dogashima 3

Dogashima 3 is made of a >50–m-thick, weakly stratified andesite breccia. The breccia comprises coarsely porphyritic andesite clasts in a white pumice sandstone matrix (Table 2). It is mostly preserved in the northern part of the area; a 5-m-thick remnant occurs at the top

315 of locality C (Fig. 2c). Its upper boundary has not been identified due to vegetation cover
316 and/or erosion.

317

318 *Grain size and components of Dogashima 2 at locality G-east*

319 The coarse (modes mostly >2 mm) grain size fraction of 10 nested (assemblage of images at
320 different magnifications) samples from D2-2 to D2-6 at locality G-east has been documented
321 with image analysis and functional stereology (Jutzeler et al. 2012) to quantify the grain size
322 distribution in volume and weight percent (Fig. 13). Three samples (base, middle, top) were
323 analysed from bed D2-3e where Cashman and Fiske (1991) identified good hydraulic sorting.

324 Samples from the massive grey andesite breccia at the base (D2-2) to the middle of the D2-3
325 pumice breccia (D2-3e base) show normal size grading in dense components (Fig. 13a),
326 whereas beds D2-3 c-d and D2-3e are reversely graded in pumice clast size. Dense clasts
327 decrease continuously in abundance from the basal unit D2-2 (50 vol. %) upwards to unit D2-
328 5 (<10 vol.%; Fig. 13c), and are more abundant (20 vol.%) in D2-6. Pumice clasts are almost
329 absent (<5 vol.%) in unit D2-2, but make up to 20–30 vol.% of the overlying pumice breccia
330 units. The matrix and cement (<2 mm) proportion ranges between 50–80 vol.%. Coarse (>16
331 mm) clasts are abundant only in the lower part of the succession (D2-2; 40 vol.%), and their
332 volume decreases to <5 vol.% in D2-2; they form a small percentage of the clasts (<2 vol.%)
333 in D2-6. Most units have a unimodal grain size distribution between -2 and -3 phi (4-8 mm),
334 although D2-2 is coarser (-5 phi; 32 mm) and in unit D2-3c, pumice clasts show a bimodal
335 grain size distribution (-4 and -2.25 phi; 16 and 5 mm). In the middle of bed D2-3e, the grain
336 size distribution in weight percent shows that pumice clasts are consistently coarser than
337 dense clasts (Fig. 13a).

338

A submarine channel in the Dogashima Formation

Between the southern localities A and G-east, the basal disconformity and internal architecture of Dogashima 2 indicate deposition in a palæo sea-floor channel more than 600 m wide and up to 15 m deep eroded into beds of Dogashima 1 and filled by units of Dogashima 2 (Fig. 11). Within the channel, the massive grey andesite breccia (unit D2-2) is especially thick and has a fully gradational to sharp contact with the overlying pumice breccia (unit D2-3, localities B, C and F). Further north (localities G-east to I), the overbank setting is characterised by much thinner (<1 m), finer grained and commonly stratified pumice breccia (D2-3) and cross-bedded pumice breccia-conglomerate (D2-6). In particular, the coarse grey andesite clasts and the massive grey andesite breccia (unit D2-2) are absent. At locality A, Dogashima 1 pinches out, reducing from ~10 m to <3 m thick, and the massive grey andesite breccia (D2-2) is thinner (at the expense of D2-1) where it onlaps the constructional morphology of the Matsuzaki Formation andesite (Fig. 2a).

The submarine channel floor between localities A and G-east includes two palæo-bathymetric lows. The main palæo-low occurs at localities E, F and G-east, and a less pronounced, ~5-m-deep palæo-low occurs between localities A and B (Fig. 14). A palæo-high is present between the two palæo-lows, over localities C, D and E, where Dogashima 1 is 15–25 m thicker than at localities A, F and G-east (Fig. 5). However, the difference in thickness is exaggerated on the sub-vertical cliffs by a general tilt of the whole Dogashima Formation by ~10° towards the east.

Elongate pumice clasts that show parallel orientation and/or imbrication of clast long axes (Table 3) were used as palæo-current indicators. Throughout the Dogashima area (Fig. 1), these palæo-current indicators imply an overall northeast to southwest palæo-current direction and, at locality B, an east to west current direction. The channel axis (though not known in detail) appears to have been roughly parallel to this palæo-current trend, so it is

reasonable to infer that the currents producing the palæo-currents indicators were focussed in the channel (Fig. 14). Syn-depositional normal faults in Dogashima 1 at locality D (Fig. 12f) indicate a palæo-slope towards the southwest, which is consistent with southwesterly directed palæo-currents. However, many cross beds imply opposite palæo-current directions (northeast to southwest and southwest to northeast), including some small-scale (<50 cm thick) compound (i.e. internally cross-stratified; McKee and Weir 1953; Allen 1963) cross beds in unit D2-8 (Fig. 12e). Opposite palæo-current directions are interpreted to be associated with current reflections and/or up- and down-currents within the channel, backsets, and/or anti-dunes. Pumice clasts in cross bedded and planar bedded facies do not show extensive rounding textures characteristic of abrasion in above wave-base setting (e.g. White et al. 2001; Manville et al. 2002). We interpret that Dogashima 2, and in fact all of the Dogashima Formation, was deposited in a below wave-base region where strong ocean currents occurred, consistent with a submarine channel setting. This interpretation matches the open-marine setting and absence of above-wave-base facies (e.g. conglomerate) in proximity to the Dogashima Formation.

Transport and depositional processes in Dogashima 2

Facies characteristics indicate that most units in Dogashima 2 were deposited from cohesionless, water-supported high-concentration density currents (e.g. Lowe 1982; Mulder and Alexander 2001; Talling et al. 2012). The units are laterally extensive, non- or weakly normally graded, and clast supported, and clay and silt matrix is very minor (<5 vol. %). Many contacts are erosive, and outsized, dense clasts are common. This transport mode lies within the spectrum of “high-density turbidity currents” of Lowe (1982). Similar density currents have also be named “high-density turbulent flows” by Postma et al. (1988), and “concentrated density flows” by Mulder and Alexander (2001). Other modes of subaqueous

transport and deposition identified in Dogashima 2 are traction currents, rolling and sliding, suspension settling and turbidity currents (Table 2).

High-concentration density current deposits in Dogashima 2

Units D2-1 to D2-5 show an overall normal grading and a decrease in dense clasts upwards. The very thick beds of massive grey andesite breccia (D2-2) and pumice breccia (D2-3) at or near the base are tabular and laterally continuous, and have gradational contacts at locations B, C and F (within the palæo-channel). Units D2-2 to D2-3 have marked concentrations of dense clasts and thicken in topographic lows. Rounding of pumice clasts in D2-2 implies abrasion of these delicate clasts in the lower dense-clast-dominated part of the current. The overall gradational contact between the andesite breccia D2-2 and pumice breccia D2-3 strongly suggests deposition from a single, sustained density current (e.g. Kokelaar et al. 2007). The high abundance of dense grey andesite clasts in D2-2 could have resulted from (1) preferential concentration of the densest components at the base of an initially heterogeneous current producing a complementary concentration of white pumice clasts higher up, and/or (2) a temporal change in clast composition being supplied to the current from the source. Either way, clasts deposited from the current in the studied area changed from being mainly dense andesite to mainly white pumice. The basal unit D2-1 is dominated by dark andesite clasts derived from the underlying Matsuzaki Formation. These clasts were incorporated by shear-induced erosion in the lower part of the high-concentration density current that deposited units D2-2 and D2-3.

Very coarse (1-10 m) grey andesite clasts occur in local clusters in the middle and upper parts of the massive grey andesite breccia (D2-2) at all localities, and define overall coarse-tail reverse grading. The biggest clasts were probably big enough to locally modify the

transporting current, favouring deposition of other coarse clasts, In addition, size segregation could have resulted from hindered settling during flowage, excluding some of the coarse clasts from the depositional boundary layer (e.g. Sohn and Chough 1993; Sohn 1997). Temporal increase in the size of clasts may have occurred in response to an increase in current velocity (waxing current) during progressive aggradation (e.g. Kneller and Branney 1995; Branney and Kokelaar 2002; Sumner et al. 2012), and/or "gliding" of out-sized clasts between a basal laminar inertia-flow and an upper turbulent flow may have been enhanced by flow confinement in channels (e.g. Postma et al. 1988). Alternatively, the supply of material at source may have become coarser through time, thus contributing to the reverse grading.

The absence of stratification in units D2-2 and D2-3 in the centre of the channel indicates that the clast concentration was high enough to suppress turbulent segregation (e.g. Kokelaar et al. 2007; Talling et al. 2007). However, at the rim of the channel (locality G-east; Figs 9a, 11), there is a sharp contact between units D2-2 and D2-3, at least five well-graded beds separated by weak bed boundaries are present in unit D2-3, and the top of unit D2-3 is hydraulically well-sorted and bimodal in clast componentry (Figs 10, 13). These features indicate local current unsteadiness, and expansion and an increase in turbulence, which reduced the particle concentration and shear in the depositional boundary layer in the density current, promoting hydraulic sorting of the particles sedimenting from the current. Thus, the density current depositing D2-3 was affected by the uneven bathymetry. Most effects were focussed on the rim of the submarine channel, where it caused a flow transformation similar to a hydraulic jump (e.g. Komar 1971; Fisher 1983; Sumner et al. 2013). In addition, a pumice-rich lens is locally present below the dense-clast-rich unit of D2-2 at locality G-east (Fig. 11), which suggests complex deposition and by-passing currents associated with uneven palæo-bathymetry. This part of the Dogashima Formation was previously interpreted by Cashman

437 and Fiske (1991) to be the result of hydraulic sorting of clasts during fallout from a
438 submarine eruption column and/or umbrella plume.

439 The increase in pumice clast size in the pumice breccia (unit D2-3) at localities C and G-east
440 (Figs 5, 13) could be a depositional response to a flow surge (e.g. Lowe 1982; Mulder and
441 Alexander 2001), or result from a change in the grain size of clasts supplied, or reflect palæo-
442 bathymetry effects, such as proposed for the underlying units. The strong preferred
443 orientation of the coarse white pumice clasts at the top of unit D2-3e at locality G-east, was
444 probably caused by syn-depositional shear in the depositional boundary layer of the flow (e.g.
445 Branney and Kokelaar 2002). Furthermore, the size of the extremely coarse (up to ~10 m),
446 dense, grey andesite and hydrothermally altered volcanic clasts within the massive grey
447 andesite breccia (unit D2-2) and pumice breccia (unit D2-3) implies a relatively short
448 distance of transport. At locality G-east, the internal stratification and clast imbrication in the
449 planar stratified pumice breccia (D2-4) indicate the development of traction, unsteadiness or
450 turbulence, all of which are typically associated with lower clast concentrations, and this unit
451 may have been deposited from the tail or waning phase of the current that deposited units D2-
452 2 and D2-3. The fine pumice breccia unit (D2-5) is also weakly internally stratified,
453 indicating current unsteadiness. Because of its similar componentry and stratigraphic
454 proximity to units D2-3 and D2-4, it may be related to the density current that deposited the
455 underlying units D2-1 to D2-4.

456

457 *Traction currents in a submarine channel environment*

458 The upper part of Dogashima 2 (units D2-6, D2-7 and D2-8) is planar and cross- stratified,
459 and very similar to the cross-bedded, planar bedded and normally graded pumice
460 breccia/sandstone (D1-1, D1-4, D1-7, D1-9 and D1-12) in Dogashima 1. In addition, some

beds in these units contain sub-rounded white pumice clasts that indicate minor clast-clast interactions. Planar- and cross-stratification are commonly attributed to high-energy, semi-continuous traction currents that typically operate in above wave-base settings (e.g. DiMarco and Lowe 1989; Kano 1991; Allen et al. 1994; White et al. 2001). However, similar depositional structures can be formed on the deep sea-floor around submarine volcanoes and in submarine canyons or channels, or on steep slopes (Wright 2001; Gardner 2010). Widespread siliciclastic dune fields in which single dunes have amplitudes up to several m have been observed in submarine channels, and origins including tidal forces, internal waves and storm currents have been proposed (e.g. Valentine et al. 1984; Shanmugam 2008). Cross-beds in D2-6 and D2-8 locally show opposite palæo-current directions (Fig. 1; Table 3), which suggest complex sedimentation from up- and down-slope currents, and/or reflection of currents on the margins of the channel, backsets, and/or antidunes. A further consideration is that water-saturated, highly vesicular pumice clasts have a low specific gravity (~1.3; Allen et al. 2008), and are thus easily re-entrained compared to siliciclastic components of identical size (e.g. Manville et al. 2002). The angular to sub-rounded pumice clasts imply weak clast abrasion, thus does not match reworking in an above wave-base setting, where pumice clasts would be quickly rounded (White et al. 2001; Manville et al. 2002).

Other transport processes

The strongly bimodal grain size of pumice clasts versus matrix in some of the tabular, laterally extensive beds of unit D2-7 at localities H and I suggests that the coarse pumice clasts (~1 m) settled from suspension synchronously with finer-grained clasts (<2 cm), waterlogging being delayed by their large size (e.g. Allen and McPhie 2009). The overall lateral continuity, local scouring, internal grading, relatively fine grain size, and medium thickness of many beds in unit D2-7 are features consistent with lateral transport and

deposition from sea-floor-hugging, low-concentration turbidity currents (e.g. Shanmugam 2002; Piper and Normark 2009; Talling et al. 2012).

Eruption-fed vs. Resedimented facies

Clast source in the Dogashima Formation

The high abundance, high vesicularity, relatively fine size (mostly <10 cm) and overall angular shape of all types of pumice clasts in the Dogashima Formation imply they are pyroclasts. The coarsest white pumice clasts (>30 cm) have remnants of quenched margins, implying quenching with seawater. The still-hot clasts of grey andesite, many with quenched margin remnants (Fig. 3b,c), and some with fluidal shape (Fig. 10a,b), indicate brecciation of a hot magma body (active lava, dome, crypto-dome or other intrusion) that generated a coarse, dense, monomictic clast population. The significant volume of relatively fine, highly vesicular pumice clasts in pumice breccia D2-3 and the single thick emplacement unit in the lower part of Dogashima 2 (D2-1 to D2-3), together with crystal fragments in the matrix, indicate that the succession D2-1 to D2-3 was directly fed by an explosive eruption. Shard-rich siltstone units in Dogashima 1 (D1-6, D1-10) also strongly attest to a pyroclastic origin. In contrast, clasts derived from probable autobrecciation and/or quench fragmentation of lava include the coarsely porphyritic andesite clasts of Dogashima 3 and the dark andesite clasts resedimented from the Matsuzaki Formation.

Style of the eruption that produced Dogashima 2

The thickness and grainsize of the D2-1 to D2-3 sequence indicate that this part likely represents the highest magnitude eruption amongst the units of the Dogashima Formation. As a result of confining pressure which reduces magmatic volatile exsolution, subaqueous

magmatic volatile-driven explosive eruptions are inherently weaker than their subaerial counterparts (Head and Wilson 2003; Allen et al. 2008; Allen and McPhie 2009). In addition, rapid quenching and waterlogging of hot pumice clasts and condensation of steam promote eruption column collapse (Allen et al. 2008). The overall inferred transport in water-supported pumice-rich density currents, normal density grading through units D2-1 to D2-3, and the presence of suspension deposits (D2-7) show strong similarities with the products of 'neptunian' eruptions as defined by Allen and McPhie (2009). However, the high abundance of originally hot dense grey andesite clasts in D2-1 (0-60 vol.%), D2-2 (>90 vol.%) and D2-3 (>20 vol.%) indicates a close association with a still-hot, co-magmatic lava dome. In addition, the coarseness of the dense clasts within the D2-3 pumice breccia suggests that collapse and quenching occurred from relatively low heights within the eruption column and at only moderate eruption intensities, favouring transport in a single density-stratified density current. The presence of scattered large dense grey andesite clasts within D2-3 indicates the proximity of the Dogashima exposures to the vent and that destruction of the dome continued during deposition of the pumice-rich facies.

Below wave-base, eruption-fed pyroclastic pumice-rich facies

The lower units (D2-2, D2-3) of Dogashima 2 have been previously interpreted as being the products of a pyroclastic eruption (Fiske 1969; Cashman and Fiske 1991; Tamura et al. 1991). The most direct evidence for an eruption-fed origin is that dense grey andesite clasts in D2-1 and D2-2 were hot on emplacement (Tamura et al. 1991). The presence of similar scattered coarse grey andesite clasts in the overall gradationally overlying pumice breccia (D2-3) implies that it is also eruption-fed. The characteristics of D2-3 can thus be taken to reliably indicate an explosive eruption-fed origin, confirming previous work aimed at identifying such facies (e.g. Cas and Wright 1991; McPhie et al. 1993; Kano et al. 1994,

1996; Kano 1996, 2003; Schneider et al. 2001; McPhie and Allen 2003). The characteristics of explosive-eruption-fed facies include (1) very thick and extensive beds emplaced by density currents reflecting the rapid aggradation of a relatively large volume of pyroclasts; (2) being mainly composed of pyroclasts of uniform texture, mineralogy and composition; (3) the dominant clasts are moderately to highly vesicular, reflecting the role of magmatic volatiles in fragmentation; (4) the dominant clasts and overall grain size are relatively fine (coarse ash to lapilli); (5) the dominant clasts are angular; some may have complete or partial quenched margins; clasts surfaces may be curviplanar and/or ragged.

The planar stratified pumice breccia (D2-4) has a gradational lower contact with D2-3. This context implies that it was also eruption-fed even though it is only moderately thick and planar stratified, both of which suggest that the clast supply and aggradation rates were less extreme than for D2-3. On the basis of context, the fine pumice breccia D2-5 is likely to be eruption-fed though probably related to a weaker eruption or eruption pulse, because it is planar stratified and relatively fine and thin (Table 2), and the proportion of dense clasts is lower than in the units below.

Three units of Dogashima 1, the pumice breccia D1-2, D1-5 and D1-11, do not contain grey andesite clasts but are otherwise very similar to D2-3 and have characteristics that strongly suggest they were also explosive eruption-fed. They are unstratified, widespread, and graded, implying deposition from subaqueous density currents, and mainly composed of fine, angular white pumice and crystal fragments.

By their thickness, lateral extent, grading, and large volume of pyroclasts (including crystal fragments), the two Kamegoiwa breccias (K1-1 and K1-2) are also considered to be deposits from high-concentration eruption-fed density currents. In addition, loose substrate from the Matsuzaki Formation was picked-up by the high-concentration density current, attesting to its

559 ability to erode. Their stratified facies are interpreted to result from interaction with uneven
560 palæo-bathymetry, in a similar way to D2-3 at locality G-east.

561

562 *Below wave-base, resedimented pyroclastic pumice-rich facies*

563 Four units in Dogashima 2 (D2-4, D2-6, D2-7 and D2-8) and five units in Dogashima 1 (D1-
564 1, D1-4, D1-7, D1-9 and D1-12) are mainly composed of highly vesicular white pumice
565 clasts identical to those in the explosive eruption-fed pumice breccia D2-3. These units are
566 internally planar bedded or cross bedded, not laterally continuous, and individual beds are
567 generally much less than 1 m thick. Importantly, the white pumice clasts are sub-rounded to
568 rounded in many of these units. The dominance of relatively fine pumice clasts indicates a
569 link to a subaqueous, magmatic volatile-driven explosive eruption, as for D2-3. However, in
570 these nine units, rounding and sorting of pumice clasts, and the relatively thin, well-bedded
571 depositional units indicate that aggradation was intermittent, and involved relatively dilute,
572 small-volume modes of transport, chiefly producing multiple, stratified, thin beds. These
573 units are interpreted to be the products of down-slope resedimentation from more proximal,
574 primary pumice-rich facies (e.g. McPhie et al. 1993; Manville et al. 1998; Wright and
575 Gamble 1999; Allen and Freundt 2006; Gardner 2010). The presence of resedimented facies
576 interbedded with eruption-fed units throughout the Dogashima Formation indicates that syn-
577 and/or post-eruption resedimentation was an important process. Interestingly, these units are
578 not significantly more polymictic than eruption-fed facies, representing (surficial?)
579 resedimentation of pumice-rich deposits from further upslope that had already been
580 hydraulically sorted.

581 Comparison of resedimented and eruption-fed facies in the Dogashima Formation indicates
582 that resedimentation involved small-volume, surficial, unconsolidated deposits, and generated

multiple sedimentation pulses, probably over large time scales, producing small-volume units bounded by sharp erosional surfaces. Given the long-time scales available for resedimentation, the total thickness (and volume) of resedimented units at the scale of an outcrop or at a locality can be equal to or larger than the actual underlying eruption-fed deposits. For example, the volume ratio of eruption-fed to resedimented deposits in D1 and D2 over the mapped area is at ca. 50:50.

Mass-wasting events

Partial destruction of an edifice is likely to remobilise clasts from various origins, histories and compositions, producing a polymictic, possibly multiple-bed deposit. Several causes can generate such collapse, such as mass-wasting events, or explosive eruptions. Volcanic breccia units (D1-3 and D1-8) include numerous clast types, and basal contacts scour the underlying beds of Dogashima 1. Both units are therefore interpreted as the products of mass-wasting events, or product of partial collapse of a volcanic cone.

The very coarse, overall monomictic, weakly stratified andesite breccia of Dogashima 3 is interpreted as resedimented autoclastic breccia, derived from collapse of a dome (or near-vent lava; Jutzeler 2012). The weakly stratified pumiceous sandstone matrix in Dogashima 3 is interpreted to have been deposited after the andesite clasts, from raining down and filtering of clasts brought by marine currents through the interstices between the clasts in the unconsolidated clast-supported breccia (e.g. Gifkins et al. 2002).

Eruption narrative

The Dogashima Formation is a combination of products from explosive eruptions, dome destruction, and inter-eruptive resedimentation. From detailed facies analysis, we reconstruct

607 the various eruption and transport processes involved in the accumulation of the
608 volcaniclastic facies (Fig. 14).

609

610 *Phase 1: Explosive activity (Kamegoiwa)*

611 Kamegoiwa pumice breccia (units K1-1 and K1-2) records the lowermost known part of the
612 Dogashima Formation. The high abundance of highly vesicular, white aphyric pumice lapilli
613 and crystal fragments records deposition of at least two high-concentration density currents
614 derived from magmatic-volatile driven explosive eruptions. The magma composition being
615 different from the other clasts of the Dogashima Formation, its magmatic source and vent are
616 likely to be distinct from the overlying units. K1-2 is locally overlain (intruded?) by lavas
617 from the Matsuzaki Formation. There is a stratigraphic gap (sea level, fault, intrusions)
618 between outcrops of K1-2 and Dogashima 1.

619

620 *Phase 2: Intermittent explosive activity and resedimentation (Dogashima 1)*

621 Dogashima 1 comprises three units (D1-2, D1-5 and D1-11) that record direct deposition
622 from subaqueous, explosive eruption-fed density currents, and two units (D1-6 and D1-10)
623 that were deposited from suspension settling associated with explosive eruptions. These
624 pyroclastic units are intercalated with seven units (D1-1, D1-3, D1-4, D1-7, D1-8, D1-9, D1-
625 12; Table 2; Fig. 5) that are resedimented equivalents of the eruption-fed units. The eruption-
626 fed units are relatively thin (<3 m) and composed of highly vesicular pumice lapilli, implying
627 that the eruptions were magmatic volatile-driven though relatively small volume. There is no
628 evidence for the presence of a dome at the vent during this phase. Phase 2 is interpreted to
629 record earlier (precursory?) explosive activity to the climactic eruption recorded by D2-3.

630

Phase 3: Effusive eruption (D2-1, D2-2)

The basal units of Dogashima 2 overlie an erosional disconformity interpreted to be submarine channel in the beds of Dogashima 1. The two lowest units, D2-1 and D2-2 are breccias composed of dense grey andesite clasts that were hot at deposition. These clasts must have been derived from an active lava dome (or near-vent lava flow) that had a volume in the order of ~1x10^6 m^3 (Fig. 14b; Jutzeler 2012). The grey andesite clasts have a slightly less evolved composition than the white pumice clasts in the eruption-fed units of Dogashima 1, but the compositions are similar enough to infer that they came from closely related magmas at the same volcano, and probably the same vent. The grey andesite clasts in Dogashima 2 are dense, non-vesicular and massive (i.e. no flow bands). A white pumice clast containing a blob of dense grey andesite in D2-3e suggests very minor magma mingling in a shared conduit/vent.

Subaqueous domes and crypto-domes commonly have a poorly vesicular core and a rim that is flow banded and/or pumiceous (e.g. Gifkins et al. 2002; Goto and Tsuchiya 2004; Allen et al. 2010) although the volume of flow-banded and vesicular facies can be minor in comparison to the massive, poorly vesicular core (Goto and Tsuchiya 2004). The absence of vesicles in the grey andesite clasts suggests that the source andesite had a low volatile content. Another possibility is that the clasts came from a cryptodome sufficiently deep to prevent vesiculation. If the grey andesite clasts were derived from an intrusion, then non-juvenile clasts representing the cover ought to be present in the breccias. However, <5 vol.% of hydrothermally altered volcanic clasts occur in D2-2 suggesting that a cryptodome source is unlikely. Therefore, we favour the interpretation that a gas-poor, andesitic lava dome was extruded on the same volcano that generated the eruption-fed pumice breccia units in phase 2, and was subsequently destroyed while still hot. Dome growth probably occurred during the

pause in aggradation recorded by the disconformity at the top of Dogashima 1, although no deposit at Dogashima attest of this growth.

Phase 4: Climactic explosive pumice-forming eruption (D2-2 to D2-5)

Units D2-3 to D2-5 are thick and dominantly composed of andesitic pumice clasts and crystals fragments generated by a small-volume magmatic-volatile-driven explosive eruption. This eruption was initially dome-seated and destroyed the active lava dome (Fig. 14c). The sequence D2-1 to D2-4 shows overall normal grading in clast density and gradational contacts, reflecting continuous deposition from a single density current composed of juvenile pumice clasts and hot-dome-derived (Tamura et al. 1991) dense clasts (Fig. 14c,d). The componentry in D2-2 and D2-3 implies that the density current was first overloaded with hot dense grey andesite clasts, but gradually changed to be dominated by white pumice clasts (Fig. 14c, d). However, the current was heterogeneous enough to locally deposit a lens of pumice breccia below grey andesite breccia (Fig. 11). The very good hydraulic sorting of waterlogged white pumice clasts and dense clasts in D2-3 at the margins of the channel is the result of local increase in turbulence and flow expansion of the high-concentration density current. The planar stratified pumice breccia (D2-4) overlying D2-3 was probably deposited from the less-concentrated waning tail of the current (Fig. 14d). The fine pumice breccia (D2-5) may have been produced by an eruption similar to that responsible for D2-3, but less intense, generating a weaker and unsteady density current.

Phase 5: Resedimentation and suspension settling (D2-6 and D2-8)

The units of cross-bedded pumice breccia-conglomerate (D2-6 and D2-8) record downslope resedimentation of the freshly erupted pyroclasts from a more proximal site by strong

currents in a submarine channel. The laterally continuous bed of planar bedded pumice breccia (D2-7) that is part of this sequence comprises coarse white pumice clasts and ash settled from suspension. The pyroclasts were either erupted at the same time as the white pumice clasts of D2-3, or from a subsequent eruption.

Phase 6: Effusive eruption (Dogashima 3)

The andesite clasts in the weakly stratified, coarsely porphyritic andesite breccia of Dogashima 3 have a distinctive composition and record extrusion and disintegration of a new lava dome, such as by lava flow front or dome collapse. The lack of vesicular clasts suggests that the magma was relatively volatile-poor. The pumiceous sand that forms the matrix of Dogashima 3 was probably derived from the pumice-rich products of the main explosive eruption of D2-3, which were subsequently resedimented.

Discussion

A submarine fall deposit in the Dogashima Formation?

Cashman and Fiske (1991) interpreted the pumice breccia at locality G-east (beds D2-3d and D2-3e in this study) to be a submarine fall deposit from a submarine eruption, drawing attention in particular to the good hydraulic sorting of white pumice and dense grey andesite clasts (Figs 10c,d, 13). However, the hydraulically well-sorted facies in beds D2-3d and D2-3e is only present at locality G-east; it can be traced for no more than 10 m laterally over the hundreds of m of exposures. D2-3 pinches out at the rim of the palæo-channel and in the overbank (localities G-west, I, J; Figs 9, 11), where it is almost exclusively composed of pumice lapilli and feldspar crystal fragments. In the channel (localities A-F; Figs 1, 5), unit D2-3 is very thick, tabular and massive, contains minor lenses of coarse pumice clasts, and

703 has a gradational lower contact with the massive grey andesite breccia (D2-2), and no
704 coexistence of pumice and density-equivalent dense clasts could be detected.

705 Subaqueous fall deposits should mimic some of the major characteristics of fall deposits from
706 subaerial explosive eruption columns (e.g. Pyle 1989), including non-erosive lower contacts,
707 lateral continuity over substantial distances, and systematic thickness and grain size changes
708 with distance from source. None of these characteristics are displayed by either the interval of
709 the submarine fall deposit of Cashman and Fiske (1991) (D2-3d, D2-3e in this study) or by
710 the gradationally enclosing D2-1 to D2-3 succession. In addition, the high concentration of
711 pyroclasts present in a submarine eruption column (such as for Dogashima 2) will promote
712 formation of vertical density currents (Manville and Wilson 2004). In vertical density
713 currents, clast velocity and sorting conditions are strongly different in comparison to low
714 clast concentration, such as used for the experiments by Cashman and Fiske (1991).

715 This study shows that D2-3, and in fact much of Dogashima 2, was deposited from sea floor-
716 hugging, eruption-fed density currents in a submarine channel setting. Locality G-east occurs
717 on the rim of the submarine channel that lies between localities A and G-east. The uneven
718 palæo-bathymetry may have caused current unsteadiness and expansion that increased
719 turbulence, in a similar way to a hydraulic jump (e.g. Komar 1971; Fisher 1983; Sumner et al.
720 2013), depositing the locally stratified and hydraulically sorted facies studied by Cashman
721 and Fiske (1991).

722

723 *Production and deposition of shards*

724 The very low abundance of juvenile glass shards in eruption-fed facies of the Dogashima
725 Formation may be characteristic of the products of subaqueous explosive eruptions where the
726 column remains underwater (Allen et al. 2008; Allen and McPhie 2009) and subsequent

727 pyroclast transport occurs in water-supported density currents. A fines-poor character could
728 be due to a combination of factors such as: (1) reduced explosivity of subaqueous explosive
729 eruptions under confining pressure compared to their subaerial counterparts (Head and
730 Wilson 2003; Allen et al. 2008); (2) reduced production of shards through clast-clast
731 interactions in the eruption column and during outflow because of the higher viscosity of
732 water compared to air (e.g. White 2000); and (3) segregation and advection of fine buoyant
733 shards with low settling velocities into buoyant plumes of seawater heated by the eruption
734 and/or during lateral transport (e.g. Cantelli et al. 2008), and deposition elsewhere.

735

736 *Water-settled facies in the Dogashima Formation*

737 Shard-rich siltstone units (D1-6 and D1-10) and a bed in the planar bedded pumice breccia
738 (unit D2-7) extend tens of m laterally and best exemplifies the kind of water-settled fall facies
739 generated by subaqueous magmatic volatile-driven explosive eruptions. D1-6 and the bed in
740 D2-7 contain very coarse (~1 m) white pumice clasts. The coarse pumice clasts in these units
741 probably cooled slowly as a result of their size, and remained buoyant until sufficiently
742 waterlogged to sink, along with shards which have slow settling velocities (e.g. suspension
743 deposits, Allen and McPhie 2009). The shard-rich units D1-10 and D2-7 do not directly
744 overlie eruption-fed density current deposits; however, the distinctive componentry, bimodal
745 grain size (shards vs. coarse white pumice clasts) and lithofacies characteristics suggest they
746 are suspension deposits generated by subaqueous explosive eruptions; any related density
747 currents are inferred to have left their deposits elsewhere. The bimodal (ash and crystals vs.
748 coarse white pumice clasts) bed in D2-7 could be related to the explosive eruption that
749 formed units D2-1 to D2-5. If correct, the presence of unit D2-7 at the same site as the
750 density current deposits D2-1 to D2-5 suggests that deposition of the entire Dogashima 2
751 sequence was relatively rapid and broadly syn-eruptive. However, the presence of cross-

752 bedded pumice breccia-conglomerate (unit D2-6) immediately beneath unit D2-7 indicates a
753 time break in the eruptive activity after deposition of D2-5. Therefore, D2-7 may be related to
754 another subaqueous explosive eruption that did not produce a density current deposit at
755 Dogashima (similar to D1-10).

756

757 **Conclusions**

758 The Pliocene Dogashima Formation (4.55±0.87 Ma; Izu Peninsula, Japan) records
759 subaqueous effusive and magmatic volatile-driven explosive volcanic activity, and inter-
760 eruptive resedimentation in a below wave-base, open-marine setting. The similar bulk
761 compositions, mineralogy and feldspar compositions of the white pumice and grey andesite
762 clasts in D1 and D2 in the Dogashima Formation suggests that these components were co-
763 magmatic and erupted from the same or closely adjacent subaqueous vent(s).

764 Thermoremanent temperatures (Tamura et al. 1991), and well-preserved quenched margins
765 and fluidal textures on dense grey andesite clasts in the lower part of Dogashima 2 show
766 these clasts were hot when deposited. The high abundance of the dense grey andesite clasts in
767 the lowermost units of Dogashima 2, D1-1 and D2-2, implies that these units record
768 destruction of an active submarine andesite dome. Pumice breccia D2-3 also contains the
769 coarse, originally hot, grey andesite clasts though the dominant components are highly
770 vesicular andesitic pumice. We infer that dome destruction involved a magmatic-volatile
771 driven, subaqueous, explosive eruption. The explosive eruption fed a sea-floor-hugging
772 water-supported density current that changed in composition from being dense andesite-
773 dominated (D2-1, D2-2) to being andesitic pumice-dominated (D2-3), and from being highly
774 concentrated (D2-1, D2-2, D2-3) to more dilute (D2-4, D2-5).

775 Explosive eruption-fed, water-supported, high-concentration density current deposits are
776 recognised by their occurrence in thick and extensive depositional units that were aggraded
777 rapidly, and are dominated by an angular, relatively fine (coarse ash to lapilli), highly
778 vesicular pyroclasts of uniform texture; massive to graded units are common, and
779 stratification may be present, depending partly on substrate morphology. Local incorporation
780 of the loose substrate, erosional basal contacts, and channel-filling context are additional
781 indicators of deposition from sea floor-hugging high-concentration density currents. Other
782 units in the Dogashima Formation (e.g. K1-1, K1-2, D1-2, D1-5, D1-11), and indeed in
783 subaqueous successions elsewhere that show similar facies characteristics but lack the
784 originally hot clasts are also likely to be explosive eruption-fed subaqueous density current
785 deposits. Coarse pumice clasts and ash in overlying planar bedded pumice breccia (D2-7) are
786 also interpreted to have an explosive eruption-fed origin but one involving settling of
787 pyroclasts from suspension rather than suspension from a density current.

788 Relatively well-sorted, planar bedded and cross bedded facies between the eruption-fed units
789 are also composed of highly vesicular pumice clasts, but contain sub-rounded pumice clasts.
790 The weak rounding of clasts, relatively thin units and well bedded character indicate that
791 these facies were resedimented from more proximal, but below wave-base locations.
792 Resedimentation is a predictable consequence of the presence of a large volume of relatively
793 fine, low density pyroclasts on the sea-floor.

794 Dogashima 2 accumulated in a broad (650 x 15 m) submarine channel. The internal
795 stratification and good hydraulic sorting within the pumice breccia (D2-3) at the rim of the
796 palæo-channel (locality G-east) are attributed to local current expansion and an increase in
797 unsteadiness and turbulence from wall effects affecting the density current, and are not
798 indicative of a submarine fall deposit sensu Cashman and Fiske (1991). Well-developed

799 planar and cross stratification suggests that traction currents operated within the submarine
800 channel.

801

802 ## Acknowledgments

803 This study was supported by the Australian Research Council, and is part of the PhD thesis of
804 M.J. We thank R. Fiske, M. Ort, J.D.L. White and S.M. Gordee for helpful discussions on
805 this paper. V. Manville, K. Kano, R.A.F. Cas and R. Fiske thoroughly reviewed an earlier
806 manuscript. K.-I. Kano is thanked for his help with the fieldwork in Japan; J.M. and M.J. are
807 grateful to the Shimoda Marine Research Center (Japan) for accommodation. S. Meffre, K.
808 Goemann and P. Robinson conducted part of the chemical and geochronological analyses.

809

810

811

812 ## Figures

813 **Fig. 1** Location, geology and stratigraphy in the Dogashima Formation. **a** Simplified map of
814 the Izu Peninsula (Japan) and the Izu-Bonin arc. Thin line is the 3,000 mbsl contour. **b** Local
815 geological map of the Dogashima Formation at Dogashima, Japan; capital letters are studied
816 localities; arrows show palæo-current directions, their colours correspond to the studied unit;
817 dip symbol for syn-sedimentary faults, thick black lines for roads; dashed red lines for
818 inferred faults. On land contour (in green) spacing is 20 m.

819

820 **Fig. 2** Coastal outcrops of the Dogashima Formation.

821 **a** Onlap and interfingering contact between the Dogashima Formation and the Matsuzaki
822 Formation (M) at locality A. The formations have a regional ~10° tilt eastwards (to the right)
823 but here shows gentle primary dip to the west. Dark andesite clasts (blue arrows) of the
824 Matsuzaki Formation are present in the polymict volcanic breccia beds (D1-3 and D1-8) of
825 Dogashima 1. Massive grey andesite breccia (D2-2) has an irregular contact with the basal
826 polymict volcanic breccia (D2-1); photo courtesy S.M. Gordee. **b** Major tabular units in
827 Dogashima 1 (D1) and Dogashima 2 (D2) at locality D (Fig. 1): pumice breccia (D1-2, D1-
828 5), cross-bedded pumice breccia (D1-1, D1-12), dark-grey polymictic volcanic breccia (D1-
829 3), and massive grey andesite breccia (D2-2). Coarse white pumice clasts (white arrows) at
830 the base of the polymictic volcanic breccia (D1-3) in Dogashima 1 were eroded from
831 underlying bed D1-2. **c** Dogashima Formation at locality C (Fig. 1). Note sharp contacts at
832 the base and top Dogashima 2 (D2). Black arrows show coarse grey andesite clasts in
833 massive grey andesite breccia (D2-2), white arrow points to lens of coarse white pumice
834 clasts in pumice breccia (D2-3). Note the gradational contact between the massive grey
835 andesite breccia (D2-2) and the pumice breccia (D2-3) in Dogashima 2. Blue arrow points to
836 coarse white pumice clasts in polymictic volcanic breccia of Dogashima 1. Dogashima 3, D3.
837
838 **Fig. 3** Examples of clasts of Dogashima 2. **a** Outsize grey andesite clast (G), in the massive
839 grey andesite breccia (D2-2), overlain by pumice breccia (D2-3), locality F. Note the weak
840 columnar joints (blue arrow). **b** Outsize grey andesite clast in the pumice breccia (D2-3) with
841 well-developed quenched rim (blue arrows). **c** Sharp transition from the massive grey
842 andesite breccia (D2-2) to basal beds of the pumice breccia (D2-3). The coarse grey andesite
843 clast has a quenched rim (blue arrow), locality G-east. White pumice, P; grey andesite, G; red
844 andesite, R. **d** Coarse white pumice clasts (P) with rough radial joints (blue arrows) and much
845 smaller grey andesite (G) and red andesite (R) clasts in pumice breccia (D2-3). **e** Rare clast of

white pumice containing an elongate blob of grey andesite; contact of the two magmas is sharp. D2-3e, locality G-east.

Fig. 4 Clast analyses in the Dogashima Formation and Shirahama Group (Online Resources 1, 2). **a** Total alkalis vs. silica (TAS) diagram for clasts in the Dogashima Formation; compositional fields after Le Bas et al. (1986); Shirahama Group data from Tamura (1990, 1994, 1995). **b, c** TiO2 vs. MgO and Zr vs. SiO2 diagrams for clasts in the Dogashima Formation, compared with Shirahama Group analyses, respectively. Plotted compositions are recalculated to 100 wt.% anhydrous. D1, D2 and D3 for Dogashima 1, Dogashima 2, and Dogashima 3, respectively. **d** Microprobe analyses of rims and cores of plagioclase crystals in Dogashima 2. Compositions of plagioclase phenocrysts from various origins define a single trend, consistent with a co-magmatic source.

Fig. 5 Stratigraphic logs of the southern part of the Dogashima Formation (localities A to G-east), displayed north (left) to south (right). Inset shows localities and palæo-flow directions on a simplified map (Fig. 1). All log bases start at sea level; d for dense clast, p for white pumice clast.

Fig. 6 Stratigraphic logs of the northern part of the Dogashima Formation (localities G-east to I), displayed north (left) to south (right). Inset shows localities and palæo-flow directions on a simplified map (Fig. 1). Bases of logs H and I start at sea level; d for dense clast, p for white pumice clast; see Figure 5 for symbol key.

869 **Fig. 7** Kamegoiwa pumice breccia, locality K. **a** Base of Kamegoiwa pumice breccia (K1-1)
870 is strongly stratified and includes high abundance of clasts from the underlying Matsuzaki
871 Formation (blue arrow). K2-2 is coarser grained, weakly stratified, and locally reversely
872 graded. **b** White aphyric pumice (p) and crystal fragments are the dominant clast types in the
873 upper unit of the Kamegoiwa pumice breccia (K2-2). Grey banded pumice clasts (g) and
874 hydrothermally altered volcanic clasts are common. Note the near-absence of matrix.

875

876 **Fig. 8** Facies in Dogashima 1 **a** Top of the reversely graded pumice breccia (D1-5), locality
877 E. Margins of the coarse white pumice clasts are very irregular and have been quenched;
878 cauliflower textures occur in some clasts (left arrow). Image has been darkened to increase
879 contrast. **b** Reversely graded pumice breccia (D1-2), locality B, with coarse white pumice
880 clasts (blue arrow). Unit D1-2 has a discordant contact with overlying polymictic volcanic
881 breccia (D1-3 and D1-8). D1-3 and D1-8 include similar coarse white pumice clasts. **c**
882 Laminae of pyroxene crystals fragments and white pumice clasts in a stratified lens of planar-
883 bedded pumice breccia (D1-1), locality D. **d** Cross-bedded pumice breccia (D1-1), locality B.
884 Margins of coarse white pumice clasts (blue arrows) are interpreted to have been quenched. **e**
885 Polymictic volcanic breccia (D1-3), locality D. The unit contains coarse white pumice clasts
886 (beside notebook) derived from underlying pumice breccia units. **f** Polymictic volcanic
887 breccia (D1-3), locality D. Grey scoria (blue arrows), white pumice clasts (orange arrow) and
888 numerous types of hydrothermally altered volcanic clasts.

889

890 **Fig. 9** Outcrops of Dogashima 2. **a** Locality G-east. Note the sharp boundary between the
891 massive grey andesite breccia (D2-2) and the pumice breccia (D2-3), the locally graded units
892 within the lower beds of the pumice breccia (beds a to e in D2-3), and the isolated grey

andesite clast at the top (arrow 1) and in the fine pumice breccia (D2-5; arrow 2). **b** Lateral transition from the rim of the submarine channel (right) to overbank setting (left), locality G-west; this photo is a view just to left of picture a. Dogashima 1 (D1) is overlain by a relatively thin bed of pumice breccia (D2-3). D2-4 and D2-5 are stratified and partially eroded in this section. The cross-bedded pumice breccia-conglomerate (D2-6) and planar bedded pumice breccia (D2-7) overlie the entire section. Minor coarse grey andesite and hydrothermally altered volcanic clasts are present in D2-3 (blue arrow). Green arrow shows location of picture c. **c** Dogashima 2 at locality G-west, showing the rim of the submarine channel. Fine-grained facies of the pumice breccia (D2-3) overlies a disconformity with Dogashima 1 (D1). Note that unit D2-3 is relatively thin and stratified at the top (arrows); the basal polymictic volcanic breccia (D2-1) and massive grey andesite breccia (D2-2) beds are absent.

Fig. 10 a, b Elongate, fluidal-shape, grey andesite clasts in the massive grey andesite breccia (D2-2), amongst other angular clasts of grey andesite (G), white pumice (P) and red andesite (R); birds-eye view, arrow indicates inferred flow direction from clast imbrication above in the stratigraphy; locality G-east. **c** Scan of a ground rock slab from the upper part of the pumice breccia (D2-3d) at locality G-east. The coarser white pumice clasts (P) are in hydraulic equivalence (Cashman and Fiske 1991) with the finer dense clasts of grey andesite (G), red andesite (R) and hydrothermally altered volcanic clasts (H). Fine-grained components are crystals fragments. Note the absence of fine (<1/16 mm) components. **d** Photomicrograph of white pumice clasts (P) in a matrix chiefly made of crystal fragments (plagioclase, minor pyroxene), unit D2-3e; plane polarised light.

916 **Fig. 11 a** Reconstruction of the original geometry of the Dogashima Formation, which shows
917 Dogashima 2 filling a submarine channel in Dogashima 1 (localities A to G-east). The
918 submarine channel includes a palæo-high at localities C to E and two palæo-lows (localities
919 A to B; F to G-east) carved into Dogashima 1. **b** Lateral changes in Dogashima 2 from
920 localities G-west to G-east. A medium to thick, stratified bed of pumice breccia (D2-3)
921 occurs at G-west (interpreted overbank setting; left), and overlies Dogashima 1 (D1) with a
922 discordant contact. At G-east (interpreted submarine channel, right), thick beds of massive
923 grey andesite breccia (D2-2) overlie D1 with a discordant contact. Locally, a lens of D2-3
924 occurs below D2-2 (extreme right). This lateral section is interpreted to represent the rim of
925 the submarine channel carved in Dogashima 1. The logs are restricted to lower part of the
926 cliff; all logs are ~5 m apart, and start at sea level. The red arrows show the position of the
927 "submarine fallout layer" from Cashman and Fiske (1991); person in yellow ellipse for scale.

928

929 **Fig. 12 a** Normally graded beds in planar bedded pumice breccia (D2-7), locality I. Grey
930 andesite and hydrothermally altered volcanic clasts are abundant at the bases of the beds,
931 whereas white pumice clasts are concentrated at the tops (density grading). **b** Large-scale
932 planar and trough cross beds in cross-bedded pumice breccia-conglomerate (D2-6) and planar
933 beds of the planar bedded pumice breccia (D2-7), locality G-west. **c** Coarse pumice clasts
934 (orange arrows) randomly distributed in a weakly stratified matrix of pumiceous sand, in
935 planar bedded pumice breccia (D2-7), locality I. **d** Large-scale trough cross-beds (blue arrow)
936 in cross-bedded pumice breccia-conglomerate (D2-8), locality H. **e** Small-scale compound
937 (i.e. internally cross-stratified) cross-beds in through cross-bedded pumice breccia-
938 conglomerate (D2-8) at locality I. Dashed lines define beds with similar current direction;
939 white arrows give the dominant bedding plane surface; west, W; east, E. **f** Syn-depositional

940 normal faults (blue line and arrows; 75/110) cutting a very thick (>2 m) section of planar
941 bedded pumice breccia (D1-1) in Dogashima 1, locality D.

942

943 **Fig. 13** Component volume and grain size distribution of white pumice and dense clasts (grey
944 andesite and hydrothermally altered volcanic clasts) at locality G-east, in Dogashima 2. **a**
945 Grain size distribution in weight percent for pumice and dense clasts, from image analysis
946 and functional stereology (Jutzeler et al. 2012); bin at ¼ phi. **b** Stratigraphic log of the basal
947 part of Dogashima 2 at locality G-east. **c** Volume percent of clast types from image analysis.
948 **d** Volume percent for size classes, from functional stereology data. **e** Volume modes for
949 pumice and dense clasts from functional stereology data.

950

951 **Fig. 14** Model involving destruction of a subaqueous dome by a magmatic volatile-driven
952 explosive eruption; the vertical scale of the volcanic edifice is strongly exaggerated. **a**
953 Geometry of the palæo-channel just before deposition of Dogashima 2, N-S section. The
954 palæo-channel (sections A–G) and overbank locations (sections H–I) are at a lower elevation
955 than the vent. Dogashima 1, (green). Palæo-channel is centred on localities E, F and G,
956 palæo-high at C and D, and palæo-low between A and B. Matsuzaki Formation (M, blue)
957 forms a palæo-high to the south. **b** Effusive subaqueous eruption (1), producing an andesitic
958 lava dome. **c** Destruction of the hot dome by a magmatic volatile-driven explosive eruption
959 (2). Dense hot dome fragments (3) fall out rapidly. The eruption column collapses, producing
960 (4) a water-supported, subaqueous density current of grey andesite dome clasts and white
961 pumice clasts (units D2-1 and D2-2). **d** Fewer dome clasts are available, and vesicular
962 pumice clasts (5) become the dominant clast type in the collapsing eruption column (unit D2-
963 3). Dense dome clasts are concentrated near the base of the water-supported high-

concentration density current (6). Coarse pumice clasts are temporarily buoyant (7) and deposited from suspension later (unit D2-7). Waning stages of the eruption (D2-4, D2-5) and pumice resedimentation (D2-6 and D2-8) are not shown in cartoon. Red for explosive jet sustained by magmatic gases; greenish blue for water-supported region dominated by waterlogged pumice lapilli; pale blue for water-supported region with a lower concentration of finer grained clasts.

Tables

Table 1

Characteristics of clasts in the Dogashima Formation.

Table 2

Characteristics of facies in the Dogashima Formation.

Table 3

Bearing (true North) of long axes of elongate pumice clasts, interpreted to be deposited parallel to flow direction, in Dogashima 1 and 2. Flow direction inferred from clast imbrication. Dip direction of syn-depositional faults indicates palæo-downslope direction.

Online Resource 1

Major and trace element compositions analysed by XRF for various clasts of the Dogashima and Matsuzaki formations. Concentrations recalculated to 100 wt.% anhydrous.

Online Resource 2

Composition of major elements in plagioclase phenocrysts and microlites in white pumice and grey andesite clasts in Dogashima 2; analysed on a Cameca 100X electron microprobe.

Online Resource 3

U/Pb analyses on zircons by LA-ICP-MS; data and Concordia.

References

Allen JRL (1963) The classification of cross-stratified units, with notes on their origin. Sedimentology 2:93-114

Allen JRL, Friend PF, Lloyd A, Wells H (1994) Morphodynamics of intertidal dunes: a year-long study at Lifeboat Station Bank, Wells-next-the-Sea, Eastern England. Philos Trans R Soc, A 347:291-344

Allen SR, McPhie J (2000) Water-settling and resedimentation of submarine rhyolitic pumice at Yali, eastern Aegean, Greece. J Volcanol Geotherm Res 95:285-307

Allen SR, Freundt A (2006) Resedimentation of cold pumiceous ignimbrite into water: Facies transformations simulated in flume experiments. Sedimentology 53:717-734. doi:10.1111/j.1365-3091.2006.00790.x

Allen SR, Fiske RS, Cashman KV (2008) Quenching of steam-charged pumice; implications for submarine pyroclastic volcanism. Earth Planet Sci Lett 274:40-49. doi:10.1016/j.epsl.2008.06.050

Allen SR, McPhie J (2009) Products of neptunian eruptions. Geology 37:639-642. doi:10.1130/G30007A.1

Allen SR, Fiske RS, Tamura Y (2010) Effects of water depth on pumice formation in submarine domes at Sumisu, Izu-Bonin Arc, western Pacific. Geology 38:391-394. doi:10.1130/G30500.1

Branney MJ, Kokelaar P (2002) Pyroclastic density currents and the sedimentation of ignimbrites. Geological Society, London

Cantelli A, Johnson S, White JDL, Parker G (2008) Sediment sorting in the deposits of turbidity currents created by experimental modeling of explosive subaqueous eruptions. J Geol 116:76-93

1017 Carey RJ, Wysoczanski R, Wunderman R, Jutzeler M (2014) Discovery of the Largest Historic Silicic
1018 Submarine Eruption. Eos Trans AGU 95:157-159. doi:10.1002/2014EO190001
1019 Cas RAF, Allen RL, Bull SW, Clifford BA, Wright JV (1990) Subaqueous, rhyolitic dome-top tuff cones: a
1020 model based on the Devonian Bunga Beds, southeastern Australia and a modern analogue. Bull
1021 Volcanol 52:159-174
1022 Cas RAF, Wright JV (1991) Subaqueous pyroclastic flows and ignimbrites: an assessment. Bull Volcanol
1023 53:357-380. doi:10.1007/BF00280227
1024 Cashman KV, Fiske RS (1991) Fallout of pyroclastic debris from submarine volcanic eruptions. Science
1025 253:275-280. doi:10.1126/science.253.5017.275
1026 DiMarco MJ, Lowe DR (1989) Shallow-water volcaniclastic deposition in the Early Archean Panorama
1027 Formation, Warrawoona Group, eastern Pilbara Block, Western Australia. Sediment Geol 64:43-63
1028 Fisher RV (1961) Proposed classification of volcaniclastic sediments and rocks. Geol Soc Am Bull 72:1409-
1029 1414. doi:10.1130/0016-7606(1961)72[1409:PCOVSA]2.0.CO;2
1030 Fisher RV (1983) Flow transformations in sediment gravity flows. Geology 11:273-274
1031 Fiske RS, Matsuda T (1964) Submarine equivalents of ash flows Tokiwa Formation Japan. Am J Sci 262:76-
1032 106
1033 Fiske RS (1969) Recognition and significance of pumice in marine pyroclastic rocks. Geol Soc Am Bull 80:1-8.
1034 doi:10.1130/0016-7606(1969)80[1:RASOPI]2.0.CO;2
1035 Fiske RS, Cashman KV, Shibata A, Watanabe K (1998) Tephra dispersal from Myojinsho, Japan, during its
1036 shallow submarine eruption of 1952-1953. Bull Volcanol 59:262-275. doi:10.1007/s004450050190
1037 Fiske RS, Naka J, Iizasa K, Yuasa M, Klaus A (2001) Submarine silicic caldera at the front of the Izu-Bonin
1038 Arc, Japan; voluminous seafloor eruptions of rhyolite pumice. Geol Soc Am Bull 113:813-824
1039 Gardner JV (2010) The West Mariana Ridge, western Pacific Ocean: Geomorphology and processes from new
1040 multibeam data. Geol Soc Am Bull 122:1378-1388. doi:10.1130/B30149.1
1041 Geological Survey of Japan (2010) Seamless digital geological map of Japan 1:200,000. In: AIST GSJ (ed)
1042 Research Information Database DB084. Geol. Surv. Jpn. AIST, Japan
1043 Gifkins CC, McPhie J, Allen RL (2002) Pumiceous rhyolitic peperite in ancient submarine volcanic
1044 successions. J Volcanol Geotherm Res 114:181-203. doi:10.1016/S0377-0273(01)00284-0
1045 Gordee SM, McPhie J, Allen SR (2008) Facies mapping of volcanic and sedimentary facies of a partly extrusive
1046 submarine cryptodome, Mio-Pliocene Shirahama Group, Izu Peninsula, Japan. In: IAVCEI General
1047 Assembly, Iceland.
1048 Goto Y, Tsuchiya N (2004) Morphology and growth style of a Miocene submarine dacite lava dome at Atsumi,
1049 northeast Japan. J Volcanol Geotherm Res 134:255-275. doi:10.1016/j.jvolgeores.2004.03.015
1050 Head JW, Wilson L (2003) Deep submarine pyroclastic eruptions: Theory and predicted landforms and deposits.
1051 J Volcanol Geotherm Res 121:155-193
1052 Huchon P, Kitazato H (1984) Collision of the Izu Block with central Japan during the Quaternary and geological
1053 evolution of the Ashigara area. Tectonophysics 110:201-210
1054 Ibaraki M (1981) Geologic ages of "Lepidocyclina" and Miogypsina horizons in Japan as determined by
1055 planktonic foraminifera. In: Ikebe N, Chiji M, Tsuchi R, Morozumi Y, Kawata T (eds) IGCP-114;
1056 International workshop on Pacific Neogene biostratigraphy; 6th international working group meeting,
1057 Osaka, Japan, Nov 25-29, 1981. Osaka Mus. Nat. Hist., Osaka, Japan (JPN), p 118-119
1058 Ingram RL (1954) Terminology for the thickness of stratification and parting units in sedimentary rocks. Geol
1059 Soc Am Bull 65:937-938. doi:10.1130/0016-7606(1954)65[937:TFTTOS]2.0.CO;2
1060 Jutzeler M (2012) Characteristics and origin of subaqueous pumice-rich pyroclastic facies: Ohanapecosh
1061 Formation (USA) and Dogashima Formation (Japan). Ph.D. thesis, University of Tasmania, Hobart,
1062 Australia, Hobart, Australia
1063 Jutzeler M, Proussevitch AA, Allen SR (2012) Grain-size distribution of volcaniclastic rocks 1: A new
1064 technique based on functional stereology. J Volcanol Geotherm Res 239-240:1-11.
1065 doi:10.1016/j.jvolgeores.2012.05.013
1066 Jutzeler M, McPhie J, Allen SR (2014) Facies architecture of a continental, below-wave-base volcaniclastic
1067 basin: the Ohanapecosh Formation, Ancestral Cascades arc (Washington, USA). Geol Soc Am Bull
1068 126:352-376. doi:10.1130/B30763.1
1069 Jutzeler M, Marsh R, Carey RJ, White JDL, Talling PJ, Karlstrom L (2014) On the fate of pumice rafts formed
1070 during the 2012 Havre submarine eruption. Nat Commun 5:3660. doi:10.1038/ncomms4660
1071 Kano K-I (1983) Structures of submarine andesitic volcano - an example in the Neogene Shirahama group in the
1072 southern part of the Izu Peninsula, Japan. Geoscience Reports of Shizuoka University 8:9-37
1073 Kano K-I (1989) Interactions between andesitic magma and poorly consolidated sediments: examples in the
1074 Neogene Shirahama Group, South Izu, Japan. J Volcanol Geotherm Res 37:59-75
1075 Kano K (1991) Volcaniclastic sedimentation in a shallow-water marginal basin: the Early Miocene Koura
1076 Formation, SW Japan. Sediment Geol 74:309-321

1077 Kano K, Orton GJ, Kano T (1994) A hot Miocene subaqueous scoria-flow deposit in the Shimane Peninsula,
1078 SW Japan. J Volcanol Geotherm Res 60:1-14
1079 Kano K (1996) A Miocene coarse volcaniclastic mass-flow deposit in the Shimane Peninsula, SW Japan:
1080 Product of a deep submarine eruption? Bull Volcanol 58:131-143. doi:10.1007/s004450050131
1081 Kano K, Yamamoto T, Ono K (1996) Subaqueous eruption and emplacement of the Shinjima Pumice, Shinjima
1082 (Moeshima) Island, Kagoshima Bay, SW Japan. J Volcanol Geotherm Res 71:187-206
1083 Kano K (2003) Subaqueous pumice eruptions and their products; a review. In: White JDL, Smellie JL, Clague
1084 DA (eds) Explosive Subaqueous Volcanism. AGU, Washington, D.C., pp 213-230
1085 Kato Y (1987) Woody pumice generated with submarine eruption. Chishitsugaku Zasshi = Journal of the
1086 Geological Society of Japan 93:11-20
1087 Kneller BC, Branney MJ (1995) Sustained high-density turbidity currents and the deposition of thick massive
1088 sands. Sedimentology 42:607-616
1089 Kokelaar P, Raine P, Branney MJ (2007) Incursion of a large-volume, spatter-bearing pyroclastic density
1090 current into a caldera lake: Pavey Ark ignimbrite, Scafell caldera, England. Bull Volcanol 70:23-54.
1091 doi:10.1007/s00445-007-0118-5
1092 Komar PD (1971) Hydraulic jumps in turbidity currents. Geol Soc Am Bull 82:1477-1487. doi:10.1130/0016-
1093 7606(1971)82[1477:HJITC]2.0.CO;2
1094 Le Bas MJ, Le Maitre RW, Streckeisen A, Zanettin B (1986) A chemical classification of volcanic rocks based
1095 on the total alkali-silica diagram. J Petrol 27:745-750. doi:10.1093/petrology/27.3.745
1096 Lowe DR (1982) Sediment gravity flows: II. Depositional models with special reference to the deposits of high-
1097 density turbidity currents. J Sediment Petrol 52:279-297
1098 Manville V, White JDL, Houghton BF, Wilson CJN (1998) The saturation behaviour of pumice and some
1099 sedimentological implications. Sediment Geol 119:5-16. doi:10.1016/S0037-0738(98)00057-8
1100 Manville V, Segschneider B, White JDL (2002) Hydrodynamic behaviour of Taupo 1800a pumice: Implications
1101 for the sedimentology of remobilized pyroclasts. Sedimentology 49:955-976
1102 Manville V, Wilson CJN (2004) Vertical density currents: A review of their potential role in the deposition and
1103 interpretation of deep-sea ash layers. J Geol Soc (London, U K) 161:947-958. doi:10.1144/0016-
1104 764903-067
1105 Matsumoto R, Katayama T, Iijima A (1985) Geology, igneous activity, and hydrothermal alteration in the
1106 Shimoda district, southern part of Izu Peninsula, central Japan. J Geol Soc Jap 91:43-63
1107 McKee ED, Weir GW (1953) Terminology for stratification and cross stratification in sedimentary rocks. Geol
1108 Soc Am Bull 64:381-389
1109 McPhie J, Doyle M, Allen R (1993) Volcanic Textures. ARC- Centre of Excellence in Ore Deposits University
1110 of Tasmania, Hobart, Australia
1111 McPhie J, Allen RL (2003) Submarine, silicic, syn-eruptive pyroclastic units in the Mount Read Volcanics,
1112 western Tasmania; influence of vent setting and proximity on lithofacies characteristics. In: White JDL,
1113 Smellie JL, Clague DA (eds) Explosive Subaqueous Volcanism. AGU, Washington, D.C., pp 245-258
1114 Mulder T, Alexander J (2001) The physical character of subaqueous sedimentary density flow and their
1115 deposits. Sedimentology 48:269-299. doi:10.1046/j.1365-3091.2001.00360.x
1116 Piper DJW, Normark WR (2009) Processes that initiate turbidity currents and their influence on turbidites; a
1117 marine geology perspective. J Sediment Res 79:347-362. doi:10.2110/isr.2009.046
1118 Postma G, Nemec W, Kleinspehn KL (1988) Large floating clasts in turbidites: a mechanism for their
1119 emplacement. Sediment Geol 58:47-61
1120 Pyle DM (1989) The thickness, volume and grainsize of tephra fall deposits. Bull Volcanol 51:1-15
1121 Raos AM, McPhie J (2003) The submarine record of a large-scale explosive eruption in the Vanuatu Arc;
1122 approximately 1 Ma Efate pumice formation. In: White JDL, Smellie JL, Clague DA (eds) Explosive
1123 Subaqueous Volcanism. AGU, Washington, D.C., pp 273-284
1124 Reynolds MA, Best JG, Johnson RW (1980) 1953-57 eruption of Tuluman Volcano; rhyolitic volcanic activity
1125 in the northern Bismarck Sea. Geological Survey of Papua New Guinea, Port Moresby
1126 Rivera J, Lastras G, Canals M, Acosta J, Arrese B, Hermida N, Micallef A, Tello O, Amblas D (2013)
1127 Construction of an oceanic island: Insights from the El Hierro (Canary Islands) 2011-2012 submarine
1128 volcanic eruption. Geology 41:355-338
1129 Sawamura K, Sumi K, Ono K, Moritani T (1970) Geology of the Shimoda District; quadrangle series, scale
1130 1:50,000, Tokyo (8) No. 105. Geological Survey of Japan
1131 Schneider JL, Le Ruyet A, Chanier F, Buret C, Ferrière J, Proust JN, Rosseel JB (2001) Primary or secondary
1132 distal volcaniclastic turbidities: How to make the distinction? An example from the Miocene of New
1133 Zealand (Mahia Peninsula, North Island). Sediment Geol 145:1-22
1134 Shanmugam G (2002) Ten turbidite myths. Earth-Sci Rev 58:311-341. doi:10.1016/S0012-8252(02)00065-X
1135 Shanmugam G (2008) Deep-water bottom currents and their deposits. In: Rebesco M, Camerlenghi A (eds)
1136 Contourites. Elsevier Science, Amsterdam, Netherlands, pp 59-81

1137 Sohn YK, Chough SK (1993) The Udo tuff cone, Cheju Island, South Korea; transformation of pyroclastic fall
1138 into debris fall and grain flow on a steep volcanic cone slope. Sedimentology 40:769-786
1139 Sohn YK (1997) On traction-carpet sedimentation. J Sediment Res 67:502-509
1140 Stewart AL, McPhie J (2004) An Upper Pliocene coarse pumice breccia generated by a shallow submarine
1141 explosive eruption, Milos, Greece. Bull Volcanol 66:15-28
1142 Sumner EJ, Talling PJ, Amy LA, Wynn RB, Stevenson CJ, Frenz M (2012) Facies architecture of individual
1143 basin-plain turbidites: Comparison with existing models and implications for flow processes. 59:1850-
1144 1887. doi:10.1111/j.1365-3091.2012.01329.x
1145 Sumner EJ, Peakall J, Parsons DR, Wynn RB, Darby SE, Dorrell RM, McPhail SD, Perrett J, Webb A, White D
1146 (2013) First direct measurements of hydraulic jumps in an active submarine density current. Geophys
1147 Res Lett 40:2013GL057862. doi:10.1002/2013GL057862
1148 Talling PJ, Amy LA, Wynn RB (2007) New insight into the evolution of large-volume turbidity currents:
1149 Comparison of turbidite shape and previous modelling results. Sedimentology 54:737-769
1150 Talling PJ, Masson DG, Sumner EJ, Malgesini G (2012) Subaqueous sediment density flows: Depositional
1151 processes and deposit types. Sedimentology 59:1937-2003. doi:10.1111/j.1365-3091.2012.01353.x
1152 Tamura Y (1990) Mode of emplacement and petrogenesis of volcanic rocks of the Shirahama Group, Izu
1153 Peninsula, Japan. Ph.D. thesis, University of Tokyo, Japan
1154 Tamura Y, Koyama M, Fiske RS (1991) Paleomagnetic evidence for hot pyroclastic debris flow in the shallow
1155 submarine Shirahama Group (Upper Miocene-Pliocene), Japan. J Geophys Res 96:21779-21787.
1156 doi:10.1029/91JB02258
1157 Tamura Y (1994) Genesis of island arc magmas by mantle-derived bimodal magmatism: evidence from the
1158 Shirahama Group, Japan. J Petrol 35:619-645. doi:10.1093/petrology/35.3.619
1159 Tamura Y (1995) Liquid lines of descent of island arc magmas and genesis of rhyolites: evidence from the
1160 Shirahama Group, Japan. J Petrol 36:417-434. doi:10.1093/petrology/36.2.417
1161 Tani K, Fiske RS, Tamura Y, Kido Y, Naka J, Shukuno H, Takeuchi R (2008) Sumisu volcano, Izu-Bonin arc,
1162 Japan: Site of a silicic caldera-forming eruption from a small open-ocean island. Bull Volcanol 70:547-
1163 562
1164 Tani K, Fiske RS, Dunkely DJ, Ishizuka O, Oikawa T, Isobe I, Tatsumi Y (2011) The Izu Peninsula, Japan:
1165 Zircon geochronology reveals a record of intra-oceanic rear-arc magmatism in an accreted block of
1166 Izu-Bonin crust. Earth Planet Sci Lett. doi:10.1016/j.epsl.2010.12.052
1167 Taylor B (1992) Rifting and the volcanic-tectonic evolution of the Izu-Bonin-Mariana Arc. Proc Ocean Drill
1168 Program: Sci Results 126:627-652
1169 Valentine PC, Cooper RA, Uzmann JR (1984) Submarine sand dunes and sedimentary environments in
1170 Oceanographer Canyon. J Sediment Petrol 54:704-715
1171 Watt SFL, Talling PJ, Vardy ME, Masson DG, Henstock TJ, Huehnerbach V, Minshull TA, Urlaub M, Lebas E,
1172 Le Friant A, Berndt C, Crutchley GJ, Karstens J (2012) Widespread and progressive seafloor-sediment
1173 failure following volcanic debris avalanche emplacement: Landslide dynamics and timing offshore
1174 Montserrat, Lesser Antilles. Mar Geol 323-325:69-94
1175 White JDL (2000) Subaqueous eruption-fed density currents and their deposits. Precambrian Res 101:87-109.
1176 doi:10.1016/S0301-9268(99)00096-0
1177 White JDL, Manville V, Wilson CJN, Houghton BF, Riggs NR, Ort M (2001) Settling and deposition of AD
1178 181 Taupo pumice in lacustrine and associated environments. In: White JDL, Riggs NR (eds)
1179 Volcaniclastic sedimentation in lacustrine settings. Blackwell Science, Oxford, England, pp 141-150
1180 White JDL, Smellie JL, Clague DA (2003) Introduction: A deductive outline and topical overview of
1181 subaqueous explosive volcanism. In: White JDL, Smellie JL, Clague DA (eds) Explosive Subaqueous
1182 Volcanism. AGU, Washington, D.C., pp 1-23
1183 Wright IC (1996) Volcaniclastic processes on modern submarine arc stratovolcanoes: Sidescan and
1184 photographic evidence from the Rumble IV and V volcanoes, southern Kermadec Arc (SW Pacific).
1185 Mar Geol 136:21-39
1186 Wright IC, Gamble JA (1999) Southern Kermadec submarine caldera arc volcanoes (SW Pacific): Caldera
1187 formation by effusive and pyroclastic eruption. Mar Geol 161:207-227
1188 Wright IC (2001) In situ modification of modem submarine hyaloclastic/pyroclastic deposits by oceanic
1189 currents: An example from the southern Kermadec arc (SW Pacific). Mar Geol 172:287-307
1190 Yamada E, Sakaguchi K (1987) Stratigraphy and geological structure of the Neogene formations, southwestern
1191 part of the Izu Peninsula, Japan. Chishitsu Chosajo Geppo = Bulletin of the Geological Survey of Japan
1192 38:357-383

Figure 1

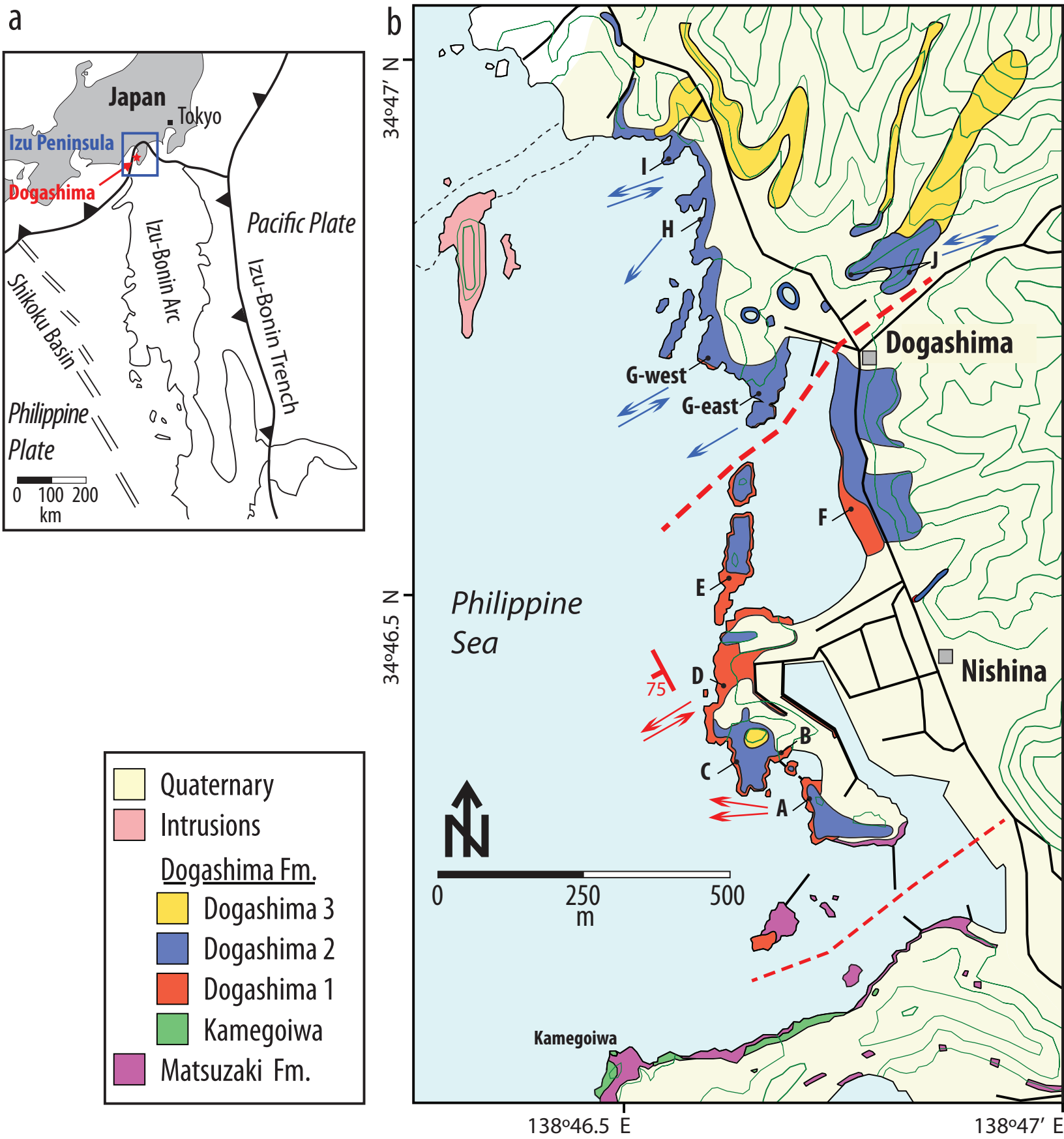
a
Japan
Tokyo
Izu Peninsula
Dogashima
Pacific Plate
Izu-Bonin Arc
Izu-Bonin Trench
Shikoku Basin
Philippine Plate
0 100 200 km
b
34°47′ N
34°46.5 N
138°46.5 E
138°47′ E
I
H
J
G-west
G-east
F
E
D
B
C
A
75
Dogashima
Nishina
Kamegoiwa
Philippine Sea
0 250 500 m
Quaternary
Intrusions
Dogashima Fm.
Dogashima 3
Dogashima 2
Dogashima 1
Kamegoiwa
Matsuzaki Fm.

Figure 2

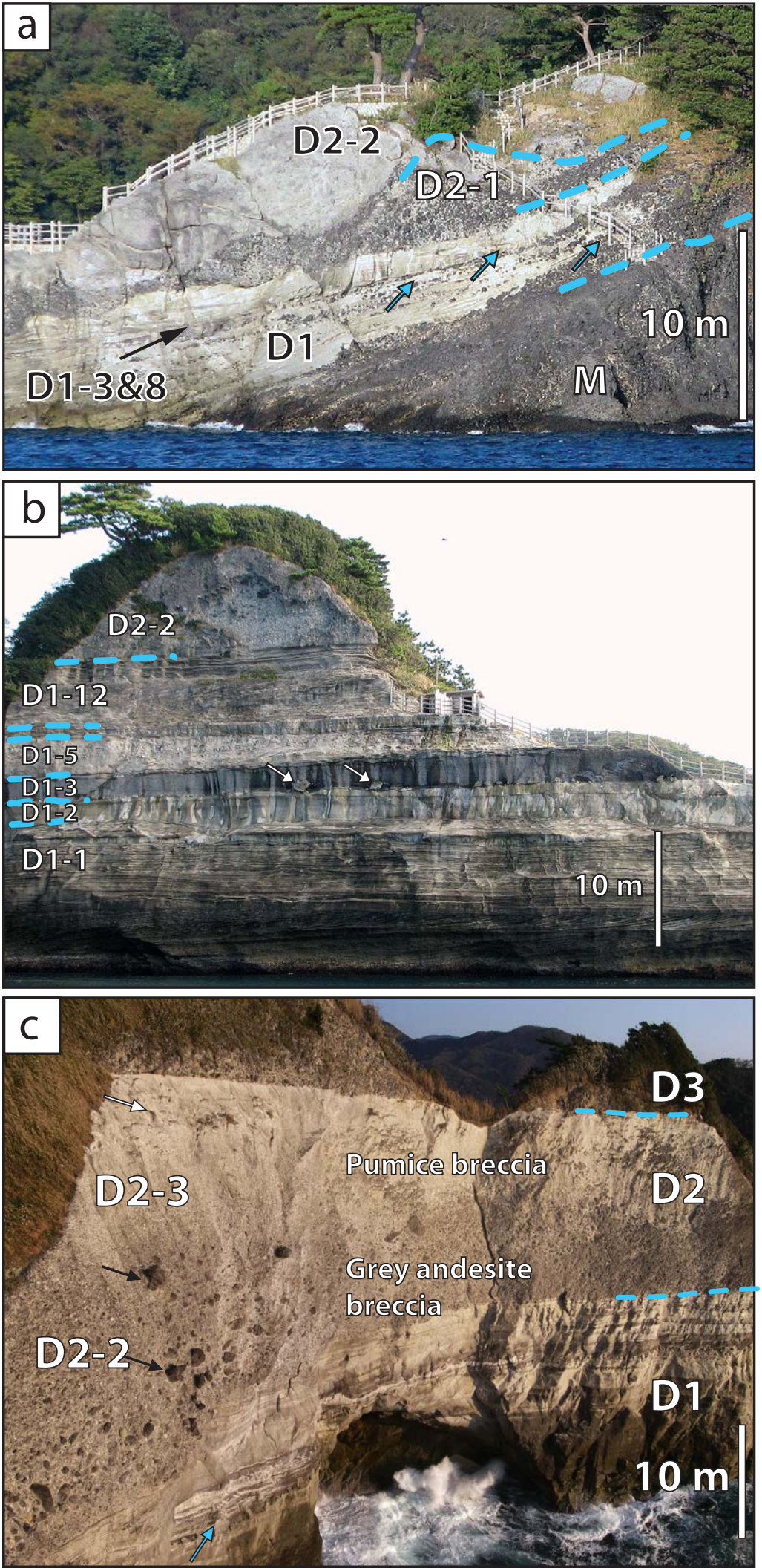
a
D2-2
D2-1
D1
D1-3&8
M
10 m
b
D2-2
D1-12
D1-5
D1-3
D1-2
D1-1
10 m
c
D3
Pumice breccia
D2-3
D2
Grey andesite
breccia
D2-2
D1
10 m

Figure 3

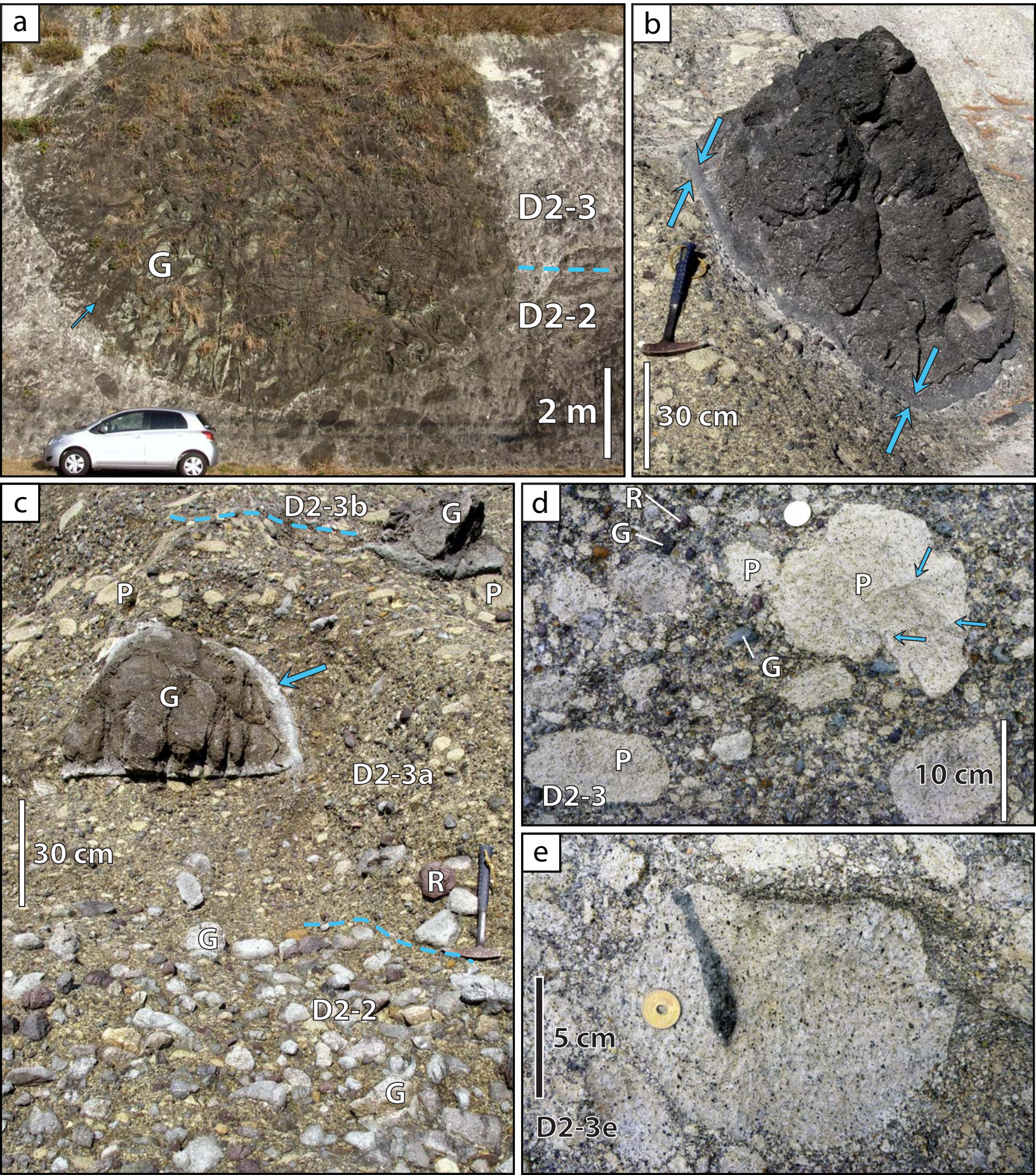
a
G
D2-3
D2-2
2 m
b
30 cm
c
D2-3b
G
P
P
G
D2-3a
30 cm
R
G
D2-2
G
d
R
G
P
P
G
P
D2-3
10 cm
e
5 cm
D2-3e

Figure 4

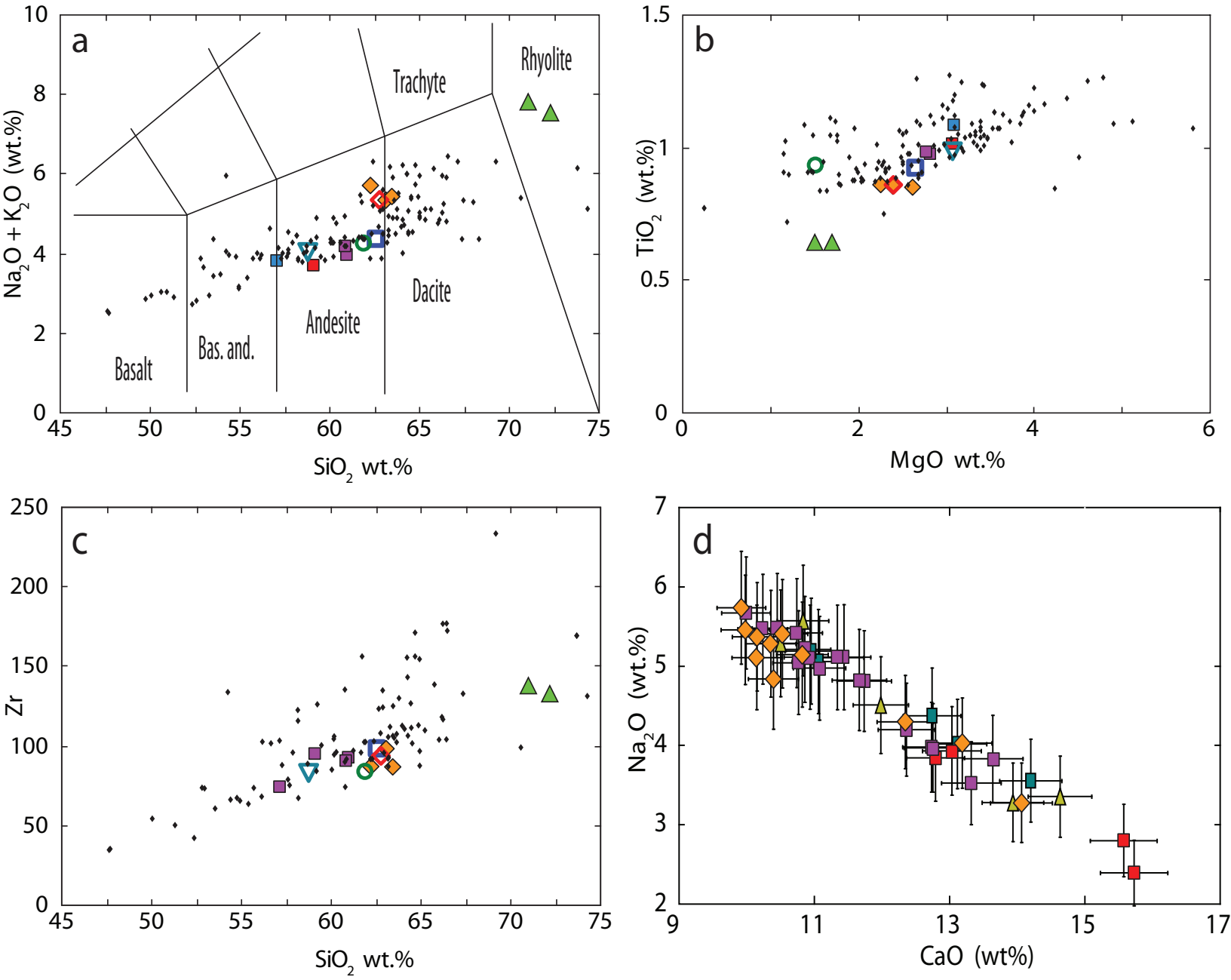
a
Rhyolite
Trachyte
Dacite
Andesite
Bas. and.
Basalt
$Na_2O + K_2O$ (wt.%)
SiO_2 wt.%
b
TiO_2 (wt.%)
MgO wt.%
c
Zr
SiO_2 wt.%
d
Na_2O (wt.%)
CaO (wt%)
White pumice D1
White pumice D2
Grey andesite D2
Red andesite D2
Inclusion in grey andesite D2
Grey andesite (microlite)
Free broken crystal
Coarsely porphyritic andesite D3
White aphyric pumice D2
Grey scoria D1
Dark andesite (Matsuzaki Fm.)
Shirahama Group

Figure 5

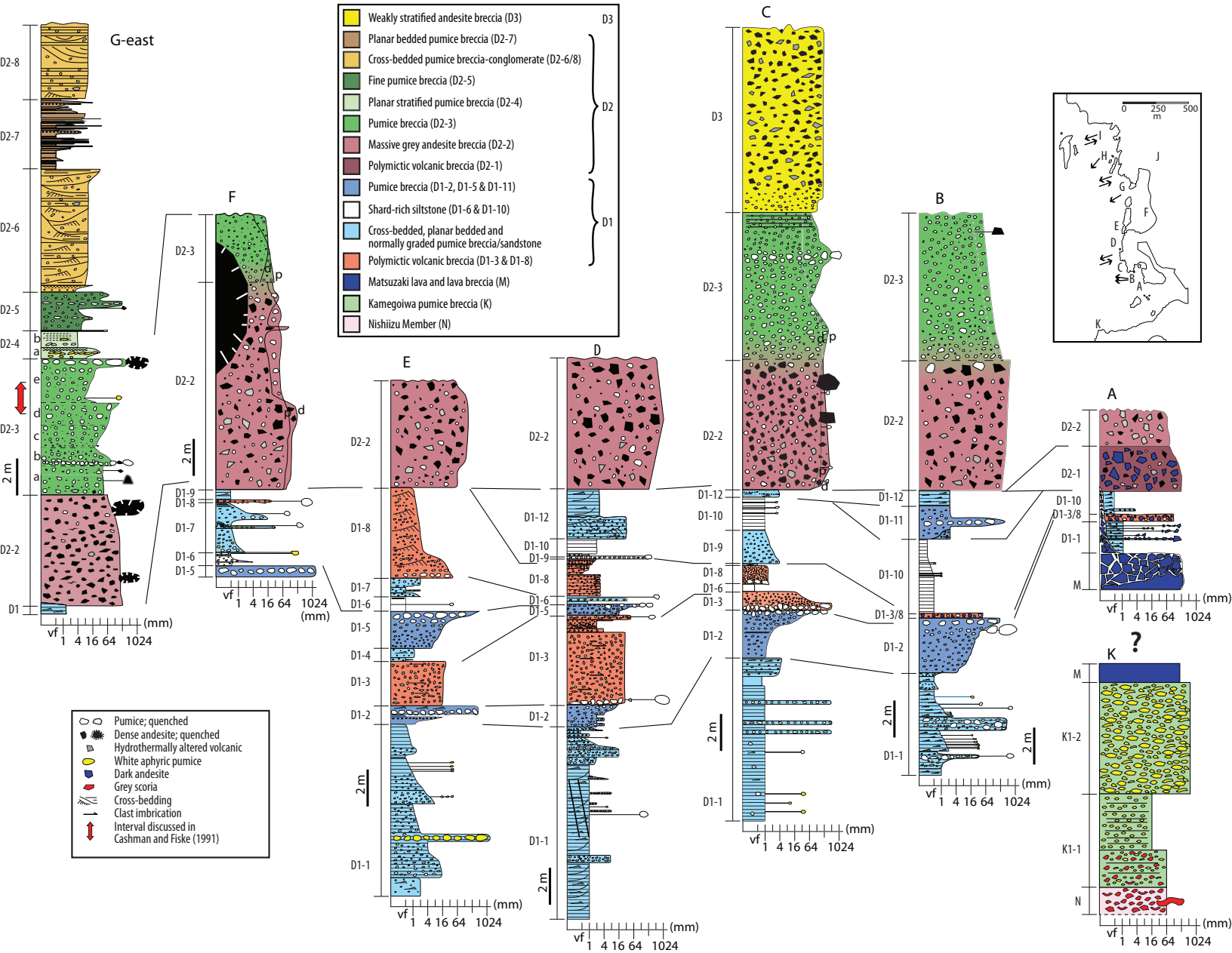
G-east
F
E
D
C
B
A
K
Weakly stratified andesite breccia (D3)
Planar bedded pumice breccia (D2-7)
Cross-bedded pumice breccia-conglomerate (D2-6/8)
Fine pumice breccia (D2-5)
Planar stratified pumice breccia (D2-4)
Pumice breccia (D2-3)
Massive grey andesite breccia (D2-2)
Polymictic volcanic breccia (D2-1)
Pumice breccia (D1-2, D1-5 & D1-11)
Shard-rich siltstone (D1-6 & D1-10)
Cross-bedded, planar bedded and normally graded pumice breccia/sandstone
Polymictic volcanic breccia (D1-3 & D1-8)
Matsuzaki lava and lava breccia (M)
Kamegoiwa pumice breccia (K)
Nishiizu Member (N)
D3
D2
D1
Pumice; quenched
Dense andesite; quenched
Hydrothermally altered volcanic
White aphyric pumice
Dark andesite
Grey scoria
Cross-bedding
Clast imbrication
Interval discussed in Cashman and Fiske (1991)
vf 1 4 16 64 1024 (mm)
2 m
0 250 500 m

Figure 6

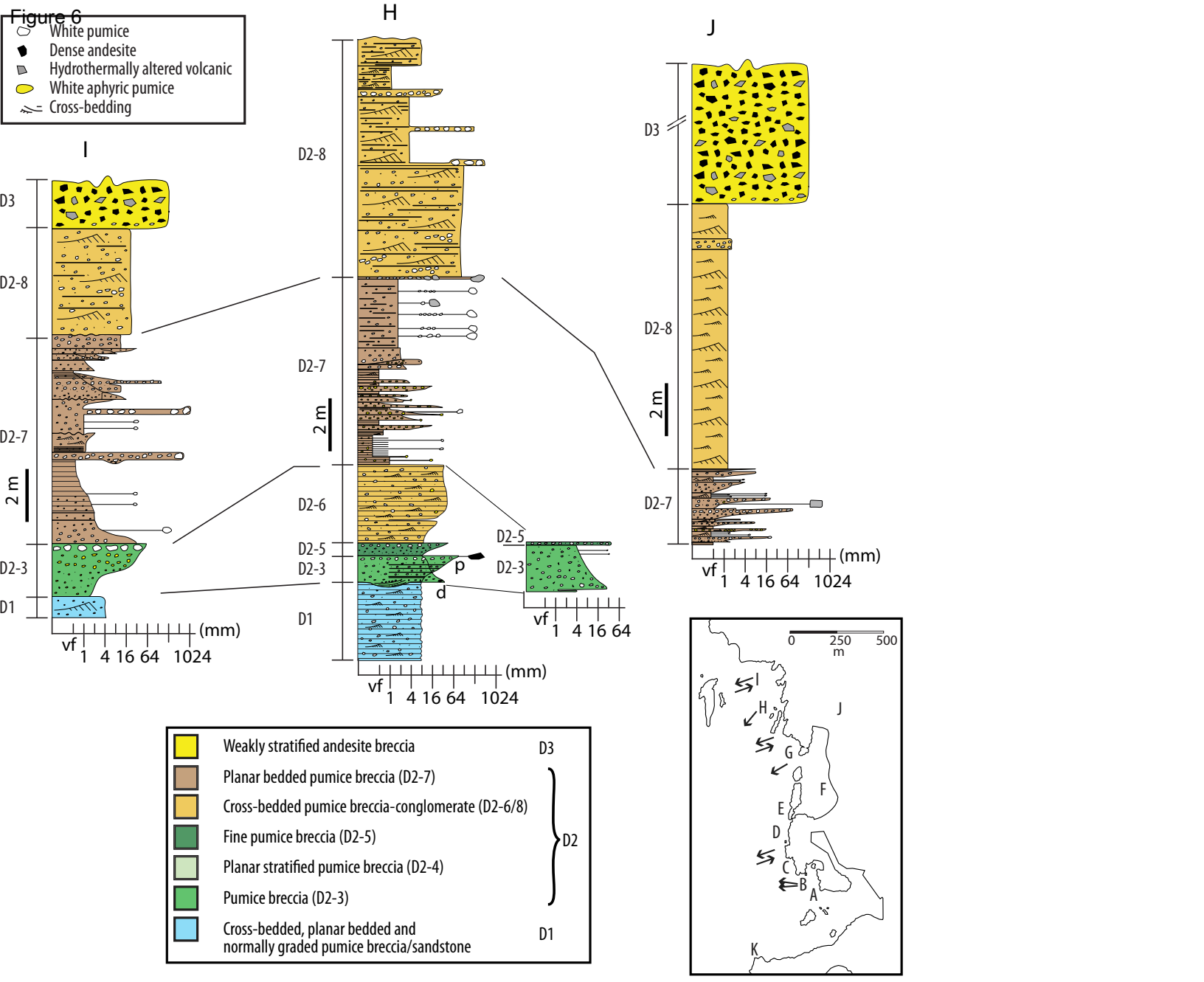
White pumice
Dense andesite
Hydrothermally altered volcanic
White aphyric pumice
Cross-bedding
I
H
J
D3
D2-8
D2-7
D2-6
D2-5
D2-3
D1
2 m
p
d
vf 1 4 16 64 1024 (mm)
Weakly stratified andesite breccia
Planar bedded pumice breccia (D2-7)
Cross-bedded pumice breccia-conglomerate (D2-6/8)
Fine pumice breccia (D2-5)
Planar stratified pumice breccia (D2-4)
Pumice breccia (D2-3)
Cross-bedded, planar bedded and normally graded pumice breccia/sandstone
D2
0 250 500 m
A
B
C
D
E
F
G
H
I
J
K

Figure 7

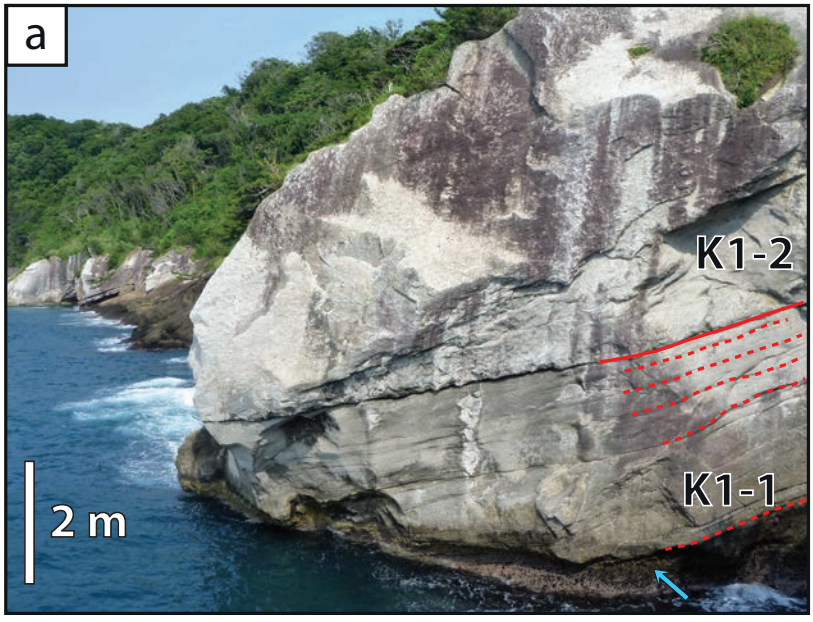

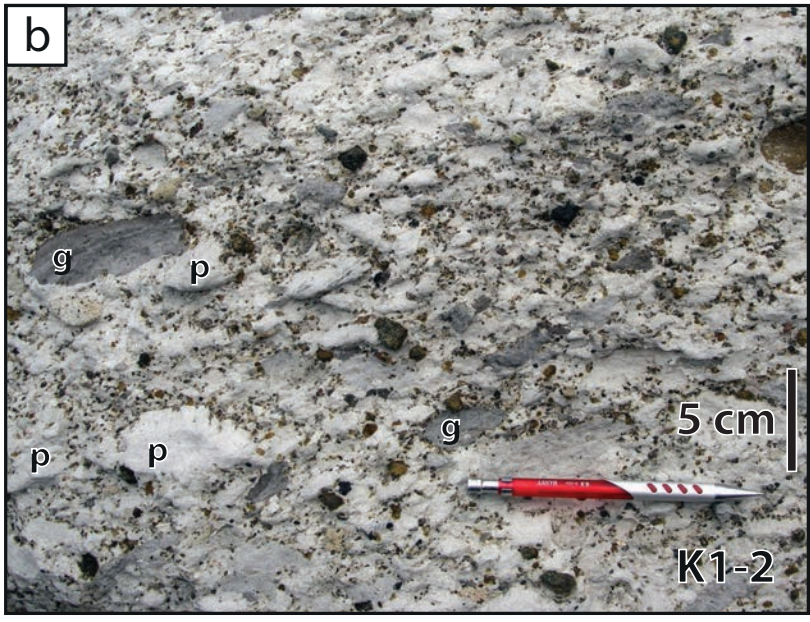

Figure 8

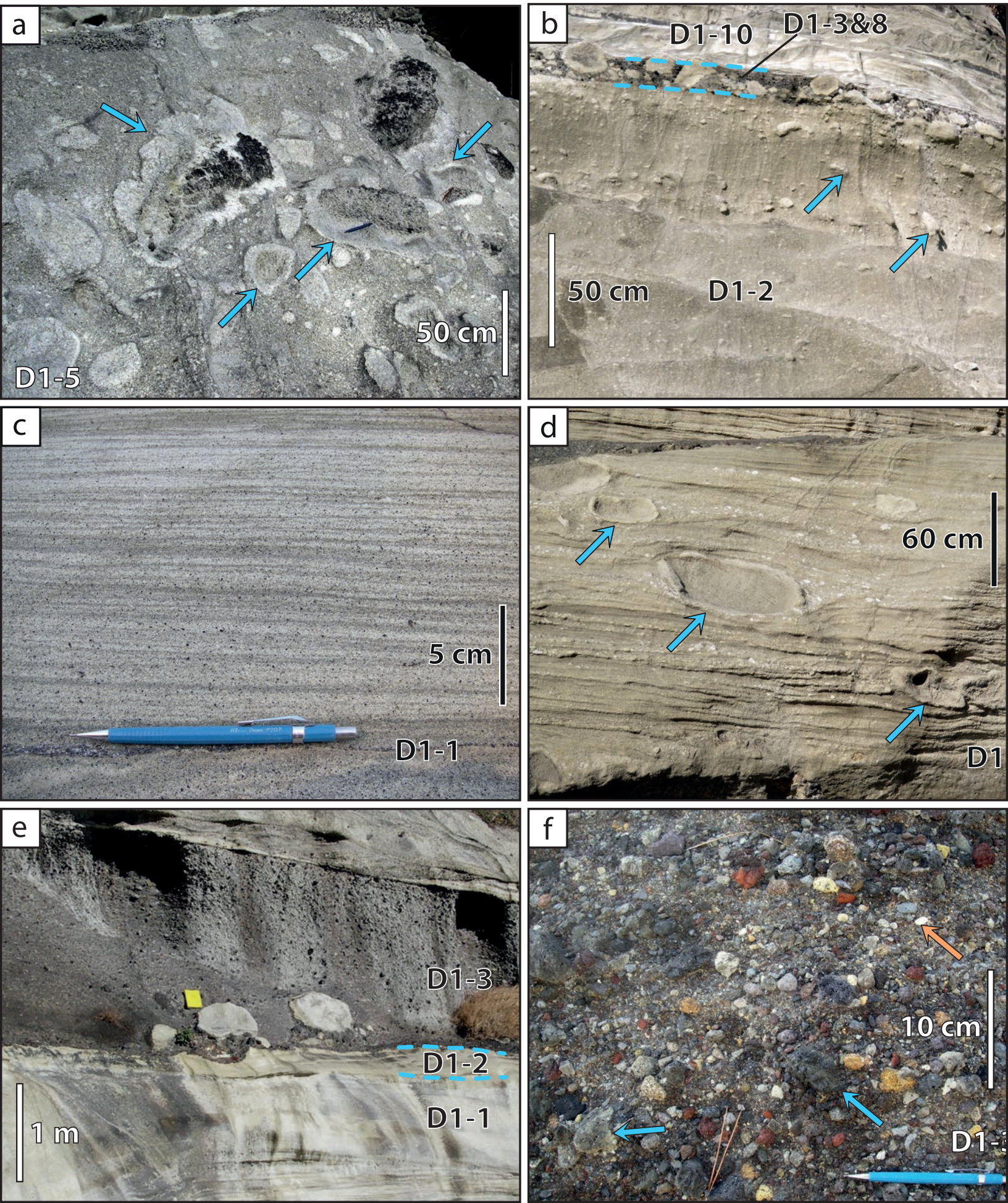
a
D1-5
50 cm
b
D1-10
D1-3&8
50 cm
D1-2
c
5 cm
D1-1
d
60 cm
D1
e
D1-3
D1-2
D1-1
1 m
f
10 cm
D1-

Figure 9

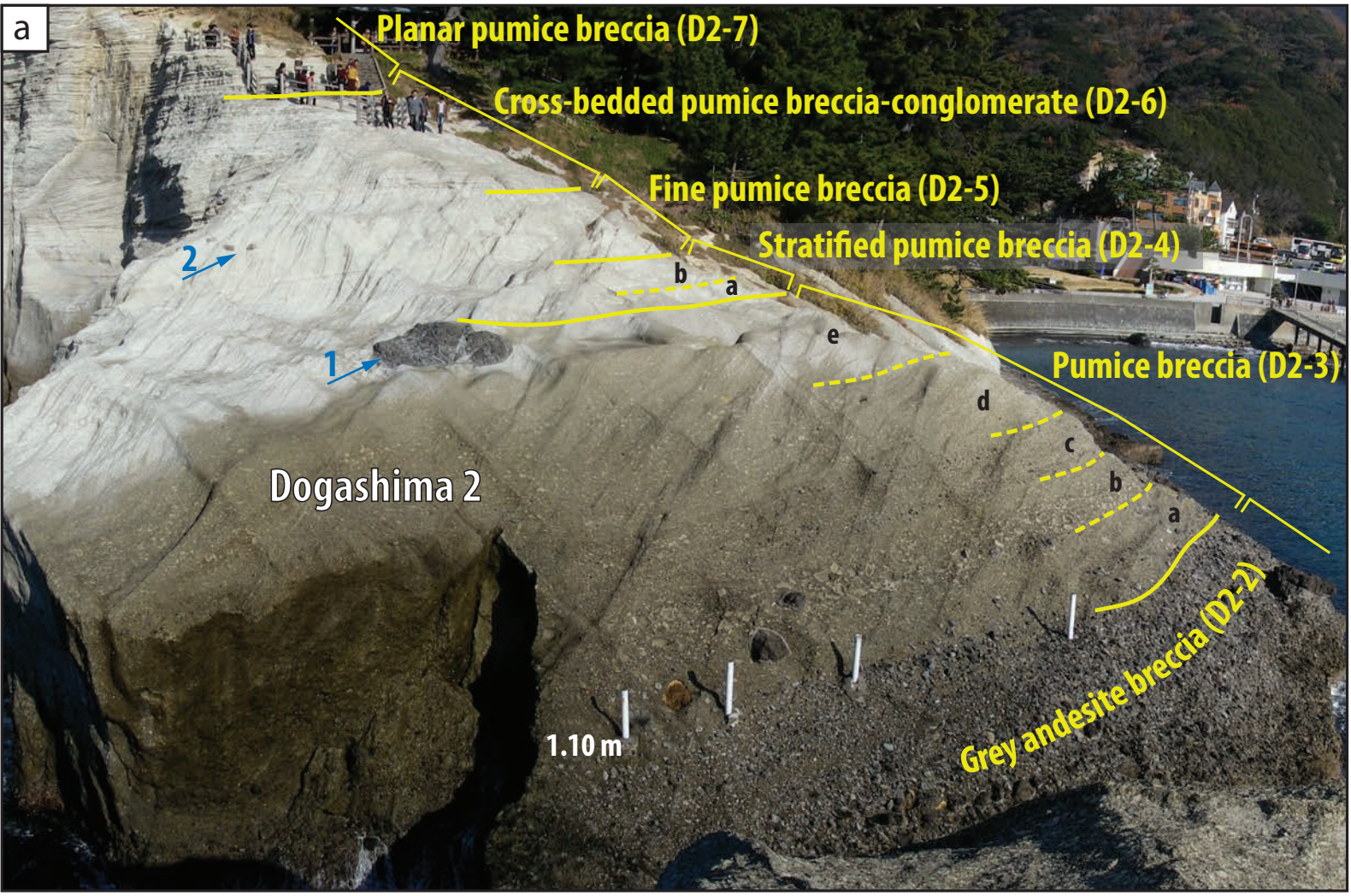
a
Planar pumice breccia (D2-7)
Cross-bedded pumice breccia-conglomerate (D2-6)
Fine pumice breccia (D2-5)
Stratified pumice breccia (D2-4)
Pumice breccia (D2-3)
Grey andesite breccia (D2-2)
Dogashima 2
1
2
a
b
c
d
e
1.10 m

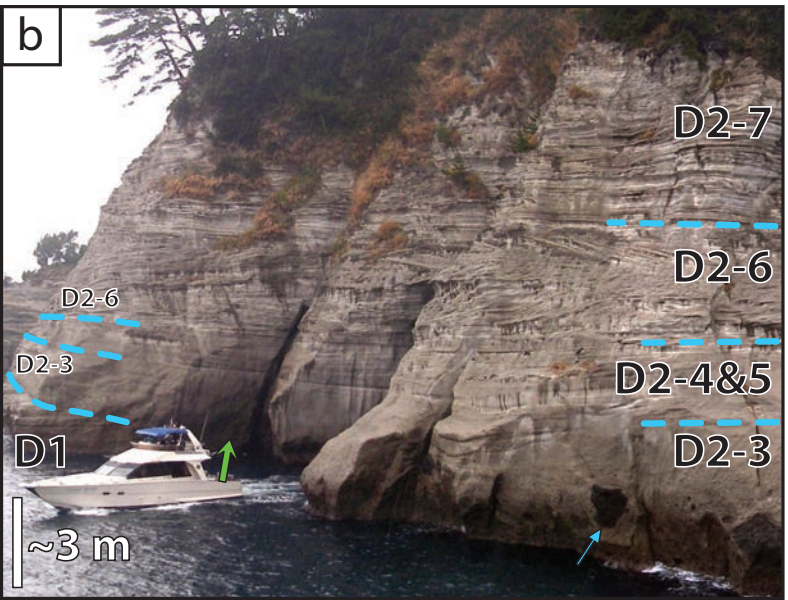
b
D2-7
D2-6
D2-4&5
D2-3
D2-6
D2-3
D1
~3 m

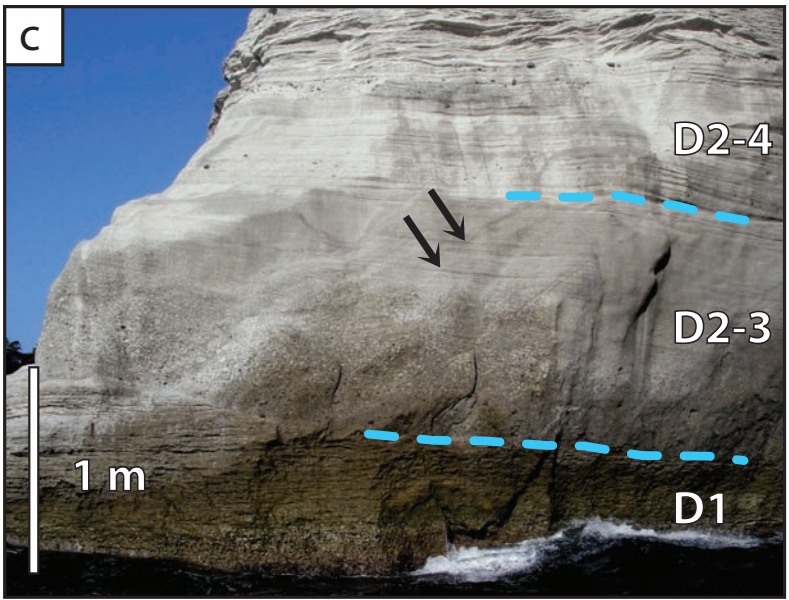
c
D2-4
D2-3
D1
1 m

Figure 10

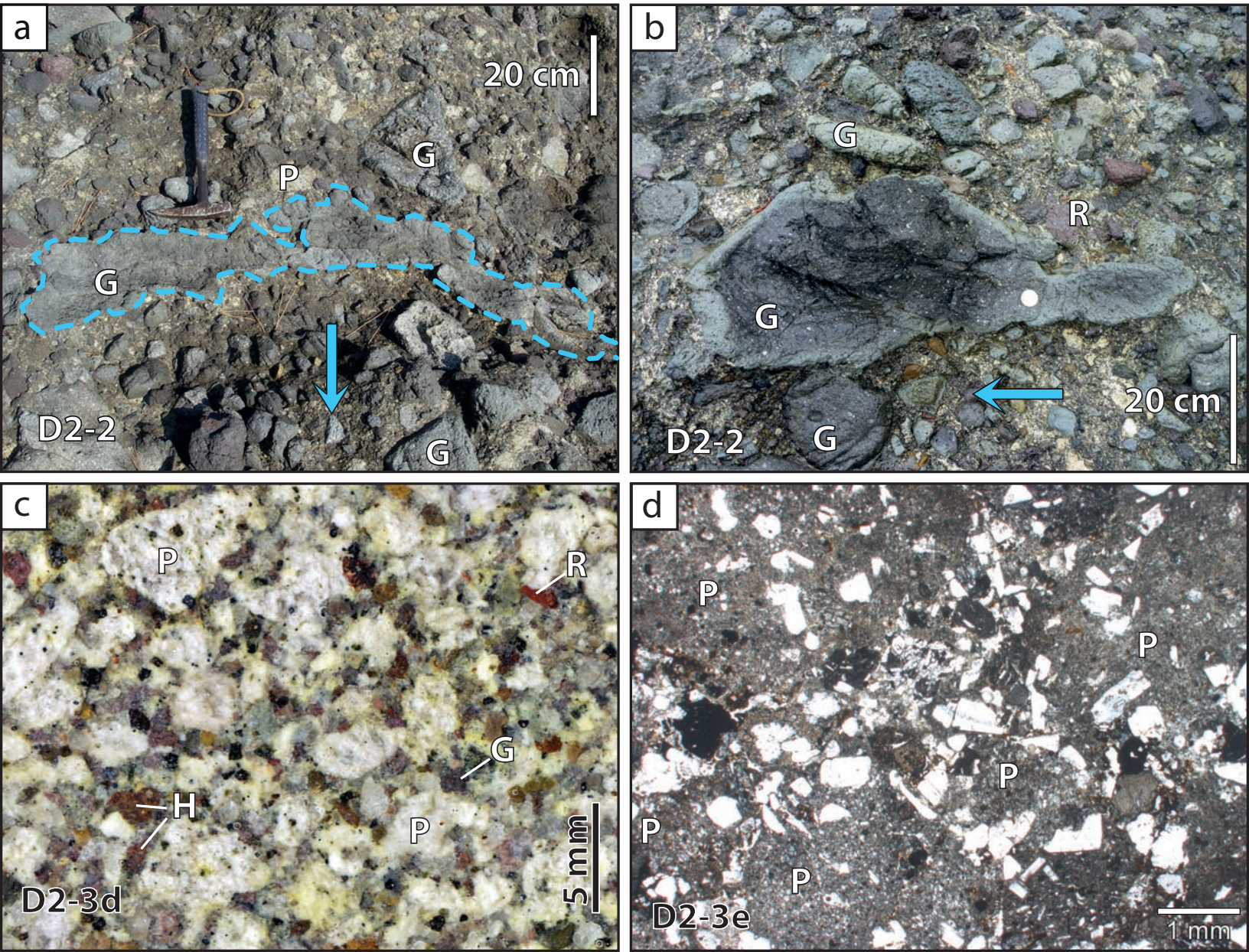
a
20 cm
G
P
G
G
D2-2
G
b
G
R
G
20 cm
D2-2
G
c
P
R
G
H
P
5 mm
D2-3d
d
P
P
P
P
P
P
D2-3e
1 mm

Figure 11

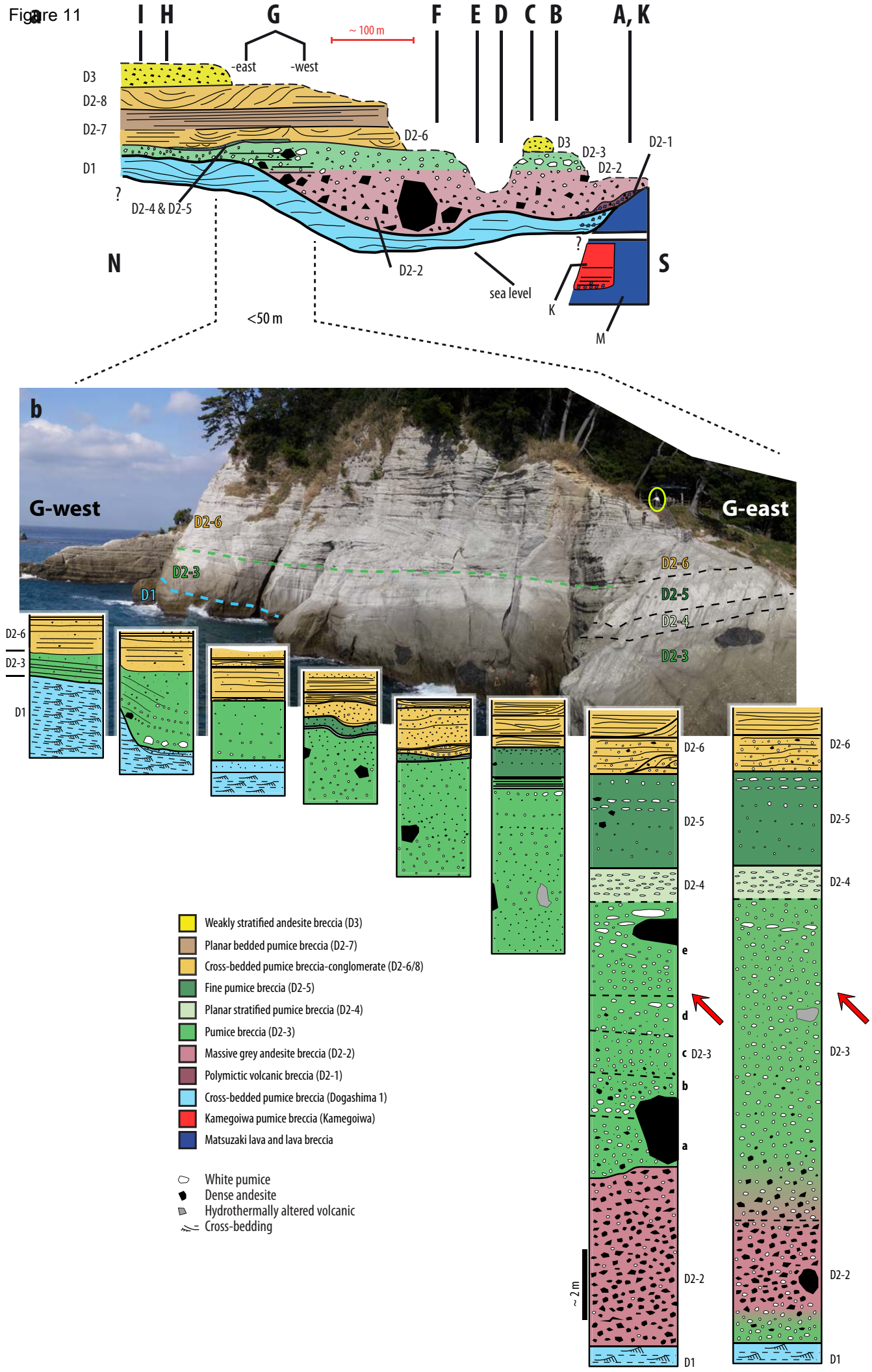
a
I H G F E D C B A, K
~ 100 m
-east
-west
D3
D2-8
D2-7
D1
D2-6
D3
D2-3
D2-2
D2-1
?
D2-4 & D2-5
D2-2
?
N
S
sea level
K
M
<50 m
b
G-west
G-east
D2-6
D2-3
D1
D2-6
D2-5
D2-4
D2-3
D2-6
D2-3
D1
D2-6
D2-5
D2-4
e
d
c D2-3
b
a
D2-2
D1
~ 2 m
D2-6
D2-5
D2-4
D2-3
D2-2
D1
Weakly stratified andesite breccia (D3)
Planar bedded pumice breccia (D2-7)
Cross-bedded pumice breccia-conglomerate (D2-6/8)
Fine pumice breccia (D2-5)
Planar stratified pumice breccia (D2-4)
Pumice breccia (D2-3)
Massive grey andesite breccia (D2-2)
Polymictic volcanic breccia (D2-1)
Cross-bedded pumice breccia (Dogashima 1)
Kamegoiwa pumice breccia (Kamegoiwa)
Matsuzaki lava and lava breccia
White pumice
Dense andesite
Hydrothermally altered volcanic
Cross-bedding

Figure 12

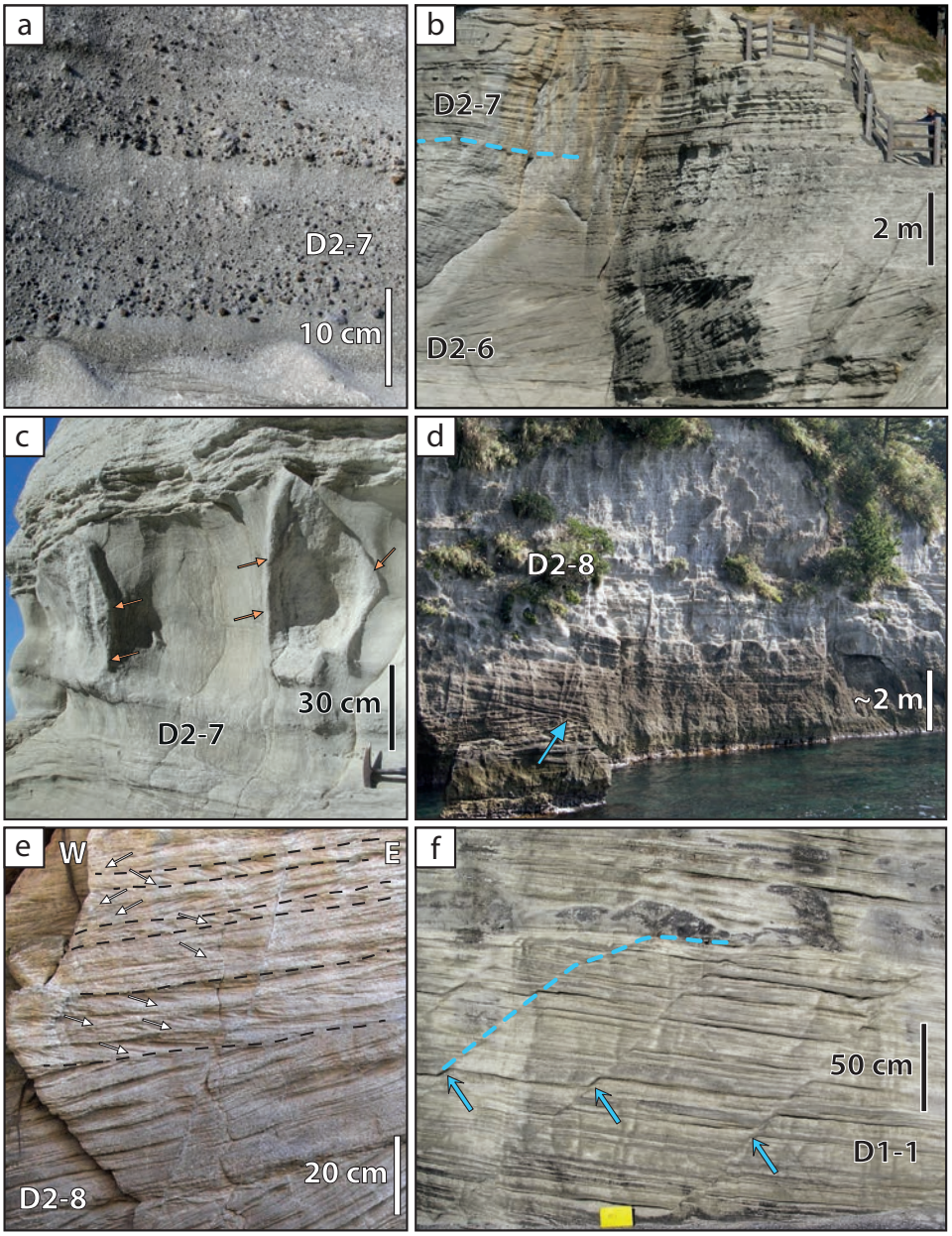

Figure 13

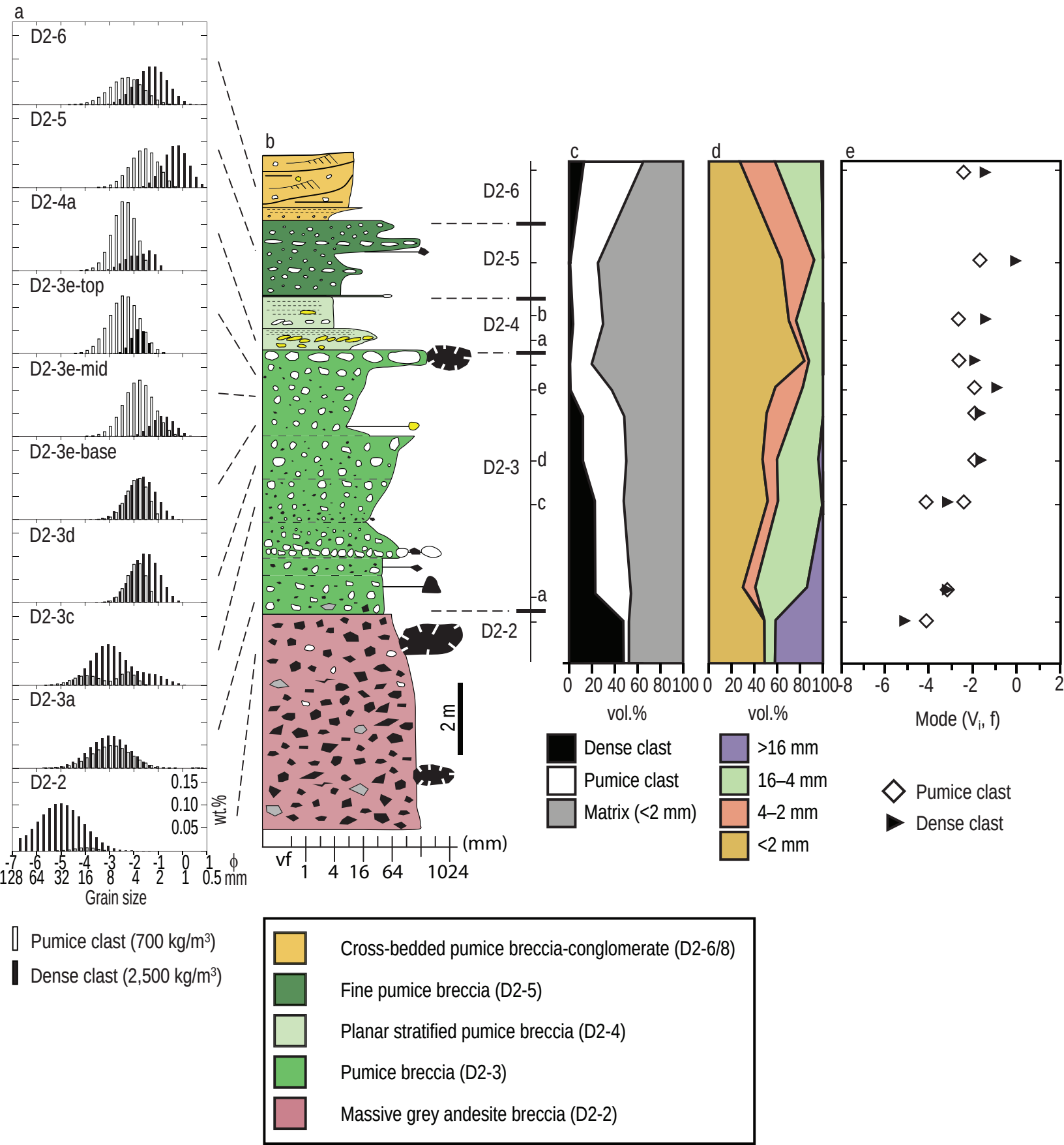
a
D2-6
D2-5
D2-4a
D2-3e-top
D2-3e-mid
D2-3e-base
D2-3d
D2-3c
D2-3a
D2-2
0.15
0.10
0.05
wt.%
-7 -6 -5 -4 -3 -2 -1 0 1 ϕ
128 64 32 16 8 4 2 1 0.5 mm
Grain size
b
D2-6
D2-5
D2-4
b
a
e
D2-3
d
c
a
D2-2
2 m
vf 1 4 16 64 1024 (mm)
c
0 20 40 60 80 100
vol.%
Dense clast
Pumice clast
Matrix (<2 mm)
d
0 20 40 60 80 100
vol.%
>16 mm
16–4 mm
4–2 mm
<2 mm
e
-8 -6 -4 -2 0 2
Mode (Vi, f)
Pumice clast
Dense clast
Pumice clast (700 kg/m3)
Dense clast (2,500 kg/m3)
Cross-bedded pumice breccia-conglomerate (D2-6/8)
Fine pumice breccia (D2-5)
Planar stratified pumice breccia (D2-4)
Pumice breccia (D2-3)
Massive grey andesite breccia (D2-2)

Figure 14

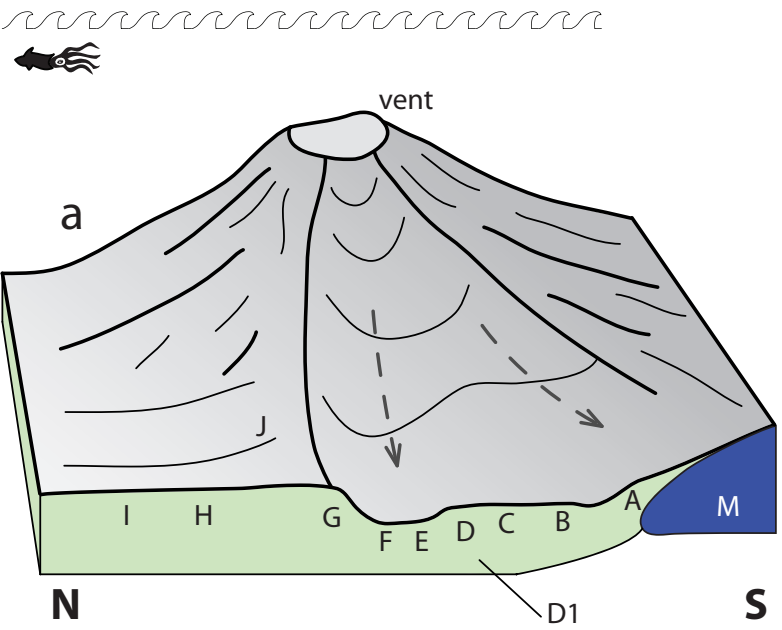

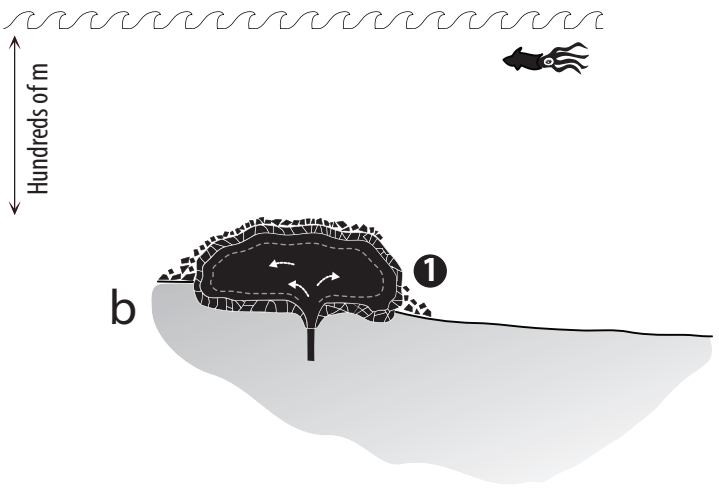

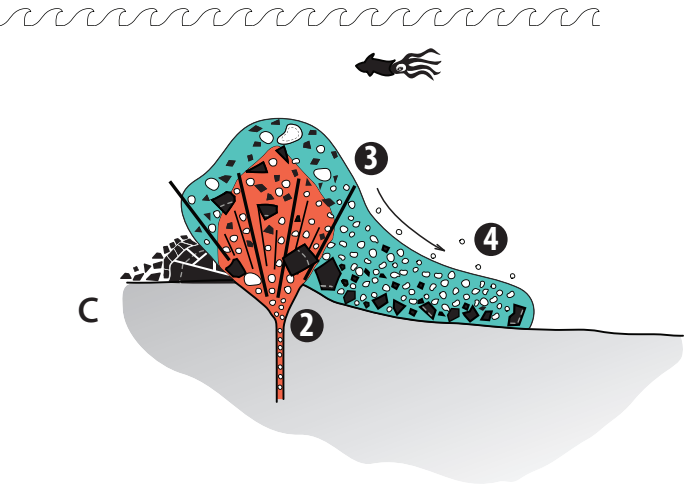

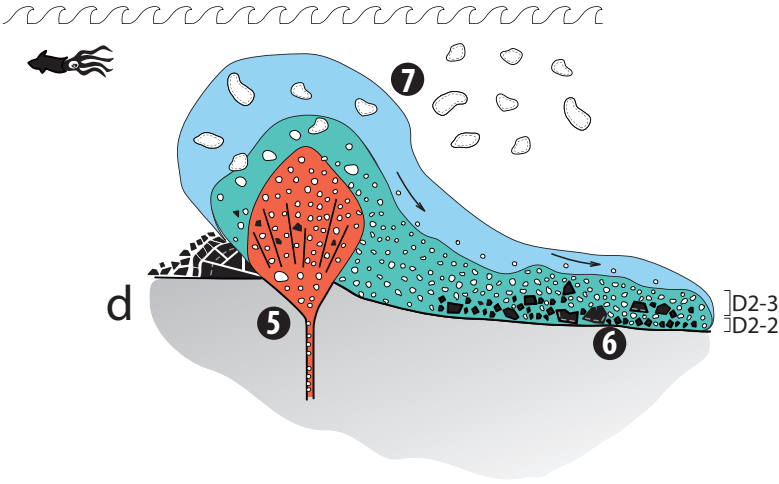

Table 1

Table Clasts in the Dogashima Formation

Clast	Occurrence	Colour; shape	Size; vesicularity	Phenocryst assemblage
White pumice	Abundant in D1 and D2, rare in base of D3	White, slight yellowish hue. Mostly angular and curviplanar, rounded in D2-2 and sub-angular to sub-rounded in D2-6 and D2-8. Common quenched rim and rare bread-crust texture in coarse (>50 cm) clasts.	Mostly <8 cm; max. 1.50 m. Elongate vesicles (>60 vol.%) partially preserved.	<40 vol.% phenocrysts. Plagioclase is dominant (25-35 vol.%, average ~1 mm, max 3 mm; An48-70). Clinopyroxene, orthopyroxene and opaque phases are subordinate (<5 vol.%) and are no more than 0.5 mm in size; quartz phenocrysts are very rare (<0.1 vol.%). Phenocrysts are equant and typically broken on one face, and are also found as clusters. Glass is chiefly devitrified.
Grey andesite	Dominant in D2, minor in lower D3	Grey to dark grey, unaltered and chiefly equant. Coarse clasts (>50 cm) are equant to ovoid, have quenched rims several cm wide and internal radial joints. Rare (<1 vol.%) fluidal clasts are present.	Mostly 10-50 cm (but up to 10 m) in D2-2; <10 cm in D2-3. Non-vesicular.	15-20 vol.% phenocrysts, which is similar to dense rock equivalent of white pumice clasts. Plagioclase crystals (10-15 vol.%; An49-57) are equant, euhedral and 1-2 mm long, although rare clusters are up to 10 mm across. Clinopyroxene (2 mm), orthopyroxene (1 mm) and oxides (1 mm) are subordinate (<5 vol.%), and form aggregates. Trachytic groundmass texture defined by 0.5-1 mm feldspar microlites (An53-69). Scattered, ovoid weakly porphyritic inclusions up to a few cm across occur.
Crystal fragments	D1 and D2	Commonly equant in shape, broken on one to many faces.	Mostly 1/16–2 mm.	Mostly plagioclase (An51-70); minor clinopyroxene and orthopyroxene.
Red andesite	D2-1, D2-2 and D2-3	Red, angular to sub-rounded, equant in shape.	Mostly <10 cm. Maximum size 30 cm. Non-vesicular	Phenocryst content and plagioclase composition (An64-78) match those of grey andesite clasts.
Hydrothermally altered volcanic clasts	D1, D2, minor in base of D3	Ochre-yellow, brown, dark red, or red; angular to sub-rounded andesite, scoria and rare sub-rounded clasts of pumice breccia.	Mostly <10 cm. Outsized (>3 m) altered pumice breccia in D2-2. Dense to formerly vesicular.	Variable mineralogy; mostly composed of plagioclase.
Dark andesite	Minor in beds of D1 at locality A and bed D1-3/8 at locality B. Dominant in Matsuzaki Fm.	Black, with brown, glassy groundmass; very angular.	Mostly 10-20 cm. Poorly vesicular (<10 vol.%).	Dominantly plagioclase and opaque phases (0.5-1.5 mm; 20 vol.%). Lath-shaped plagioclase micro-phenocrysts (0.1–0.2 mm; >50 vol.%) also occur.

White aphyric pumice	Rare to minor in some D1 and D2 beds. Dominant in Kamegoiwa and some other beds.	White, commonly rounded but angular in some beds.	Mostly <6 cm. Tube vesicles (~60-80 vol.%) overall finer and more elongate than in the white pumice.	Almost aphyric; rare plagioclase (<1 vol.%) is 0.1 mm (1 mm max). The glass is chiefly devitrified.
Grey scoria	Minor in D1-3 and D1-8. Minor in some beds of Matsuzaki Fm.	Pale grey; broken angular pieces of fluidal clasts.	Mostly <6 cm. Maximum ~10 cm. Moderately vesicular (<50 vol.%); vesicles mostly ellipsoidal, weakly aligned (<0.2 mm, max 3 mm).	Minor phenocrysts (<10 vol.%) including plagioclase (max 2 mm), clino- and orthopyroxene and rare hornblende.
Coarsely porphyritic andesite	Dominant in D3.	Grey; angular.	Almost exclusively 20-50 cm. Very poorly vesicular (<0.5 vol.%)	Phenocrysts (>25 vol.%) are mostly plagioclase (1 mm and few crystals up to 10 mm), with minor clino- and ortho-pyroxene and opaques. Groundmass is fine-grained (<0.1 mm) and composed of feldspar and subordinate clino- and ortho-pyroxene and opaques.
Grey banded pumice	Common in Kamegoiwa.	Grey, flow-banded with dark and pale domains; angular	3-12 cm long, porphyritic.	Phenocrysts (>25 vol.%, up to 3 mm) are mostly feldspath and ferromagnesians.

Table 2

Beds, occurrence	Bed characteristics	Clast characteristics	Origin
Kamegoiwa			
Pumice breccia K1-1, K1-2 Locality: K	Very thick (up to 10 m) sequence made of two stratified units separated by sharp contact boundary. K1-1 occurs locally, whereas K1-2 is present at all outcrops. The pumice breccia is in erosional contact with underlying units of the Matsuzaki Formation and lowermost beds (up to 2 m thick) contain high concentration of scoria clast picked up from the Matsuzaki Formation. The lowermost unit K1-1 (5 m) is fine stratified breccia ; K1-2 (5 m) is reversely graded, stratified pumice breccia.	Angular white aphyric pumice (>70 vol. %), sub-dominant crystal fragments, hydrothermally altered volcanic clasts (10 vol. %) and flow-banded pumice clasts (<5 vol. %). Up to 50 vol.% of grey scoria at contact with the Matsuzaki Formation. Average grain size: 1 - 2 cm (K1-1) and 1 - 16 cm (K2-2); maximum: 40 cm.	Explosive eruption-fed
Dogashima 1			
Pumice breccia D1-2, D1-5, D1-11 Localities: B, C, D, E	Thick to very thick; reversely or normally graded. Tabular, massive and in sharp contact with other units; the top contact is discordant at many localities. Contains lenses of coarse white pumice clasts.	Mostly angular white pumice (>60 vol.%), sub-dominant crystal fragment, minor angular hydrothermally altered volcanic clasts, rare white aphyric pumice (<1 vol.% clasts). Commonly consist of 20-40 vol.% of sand-sized clasts. Average grain size: 0.05 - 20 cm; maximum: 120 cm.	Explosive eruption-fed
Shard-rich siltstone D1-6, D1-10 Localities: A, B, C, D, E, F	Thin to medium. Massive to laminated; load, liquefaction-convolution (Table 1) and ball-and-pillow structures occur. Overlies other beds at sharp boundaries. The top contact is commonly an erosion surface.	Mostly devitrified glass shards; minor coarse white pumice clasts and free broken plagioclase crystals. Average grain size: <0.0063 cm.	Explosive eruption-fed
Polymictic volcanic breccia D1-3, D1-8 Localities: A, B, C, D, E, F	Medium to very thick (max 5 m); stratified, normally or reversely graded, or cross bedded. Well sorted. Tabular and laterally continuous and merge into a single <50-cm-thick coarse bed at 100 m southeastward of locality C. Basal contact is sharp, discordant and erosional; pinches out above Matsuzaki Formation at locality A. Coarse white pumice clasts can occur in D1-3, probably derived from top of D1-2.	Very angular to angular hydrothermally altered volcanic clasts, grey scoria, white aphyric pumice, white pumice, dark andesite. D1-8 rich in rounded white pumice clasts (max 40 cm). Average grain size: 0.5 - 4 cm; max. 120 cm.	Resedimented
Cross-bedded, planar bedded and normally graded pumice breccia/sandstone D1-1, D1-4, D1-7, D1-9 and D1-12 Localities: A, B, C, D, E, F	Thin to very thick (max >2 m); cross-bedded in trough or planar bedded, commonly laminated, or normally graded. Occur in stacks of low angle, lenticular sets of trough cross beds with m to 10 m wavelengths and amplitudes up to 2 m. Numerous subvertical syn-sedimentary normal faults occur in a ~2-m-thick cross-bedded pumice sandstone bed in unit D1-1 at locality D. The faults dip towards the SE, and have a vertical displacement of <20 cm.	Mostly angular to sub-rounded white pumice; minor hydrothermally altered volcanic clasts, crystal fragments, white aphyric pumice. Out-sized white pumice and white aphyric pumice clasts (both up to 1.5 m) spread throughout the beds, or concentrated in single-clast-thick beds. Scattered dark andesite clasts occur in beds in contact with the Matsuzaki Formation at locality A. Average grain size: <0.2 - 6 cm; max. 150 cm.	Resedimented

Dogashima 2

Basal polymictic volcanic breccia D2-1 Locality: A	Thick to very thick (<3 m); massive, in lense (<10 m long). Basal erosive contact that scours (1 m deep, 2 m wide) D1. Contact with overlying D2-2 is sharp and irregular.	Mostly angular dark andesite (0–60 vol.%) and grey andesite (20-30 vol.%); minor hydrothermally altered volcanic clasts, red andesite and rounded white pumice (<3 vol.%) crystal fragments. Dark andesite absent from lowermost 30 cm of the unit. Average grain size: 5 - 50 cm; max. 80 cm.	Explosive eruption-fed
Massive grey andesite breccia D2-2 Localities: A, B, C, D, E, F	Very thick (up to 7 m); massive to reversely graded. The basal contact is sharp and discordant with D1 and with D2-1 at locality A; it onlaps the Matsuzaki Formation at locality A. Minimum volume estimated at $1x10^6$ m^3.	Mostly angular grey andesite (>90 vol.%); minor hydrothermally altered volcanic clasts, rounded white pumice (up to 5 vol.%), red andesite; fluidal grey andesite (0.1 vol.%) at locality F. Outsized grey andesite clasts (up to ~10 m diameter) mainly occur in groups in the upper part of the unit at all localities. Locality F: thermoremanence of some of the coarse grey andesite clasts show deposition at >450°C (Tamura et al. 1991). Average grain size: 5 - 50 cm.	Explosive eruption-fed
Locality: G-east	Very thick; massive to normally graded, with groups of quenched out-sized andesite clasts. Basal contact is sharp and erosive with D1. Pinches out sharply at this locality.	Mostly angular grey andesite; minor hydrothermally altered volcanic clasts (<5 vol.%), rounded white pumice (up to 5 vol.%), red andesite, fluidal grey andesite (<1 vol.%). Outsized grey andesite clasts (up to ~5 m diameter) mainly occur in groups in the upper part of the unit at all localities. Average grain size: 5 - 50 cm; max. 400 cm.	
Pumice breccia D2-3 Localities: B, C, F	Very thick (6-10 m); overall massive to normally graded, with diffuse, coarse lenses of white pumice clasts. Top of unit commonly stratified. Conformable with D2-2, fully gradational. Gradational contact with D2-2 shown by high concentrations of grey andesite and hydrothermally altered volcanic clasts identical to those found in D2-2. Minimum volume estimated at $2.5x10^6$ m^3.	Mostly angular white pumice, grey andesite, crystal fragment. Minor hydrothermally altered volcanic clasts and white aphyric pumice. Average grain size: 0.2 - 60 cm; max. 120 cm.	Explosive eruption-fed
Locality: G-east	Very thick (up to 7 m); overall reversely graded and stratified into five well-preserved 1-2.5 m thick, normally or reversely graded beds separated by weak bed boundaries. Bed boundaries become less distinct upwards in the unit. Conformable with D2-2, in gradational to sharp contact. Gradational contacts are shown by decrease in size and abundance of major clasts of D2-2 in lower beds of D2-3. Coarse white pumice clasts at top of unit are aligned NE-SW. Locally, unit D2-3 can be found as a 1-m-thick lense below unit D2-2.	Dominated by angular white pumice (mostly 70-95 vol.%), grey andesite (mostly <30 vol.%) and crystal fragment. Minor hydrothermally altered volcanic clasts and white aphyric pumice. D2-3a, b are rich in grey andesite and hydrothermally altered volcanic clasts (30–50 vol.%). The base of bed D2-3b contains abundant coarse white pumice clasts as well as grey andesite clasts. Abundance of grey andesite clasts diminishes progressively in D2-3c, d, e (60 to <20 vol.% upwards). Outsized grey andesite (3.5 m) with white pumice (30 cm) in bed D2-3e; hydrothermally altered pumice breccia (1 and >3 m) in various places in base to middle of unit D2-3. Average grain size: 0.2 - 60 cm.	
Localities: G-west, H, I	Medium thick to very thick (up to 1 m), stratified. Basal contact sharp and discordant with D1. Locality G-west: medium bedded, normally graded; locality H: thickly bedded, normally graded; locality I: the 1-m-thick, reversely graded bed; lenses of coarse white pumice clasts at top.	Mostly angular white pumice (>80 vol.% of the clasts), with sub-dominant grey andesite, crystal fragment; rare outsized hydrothermally altered volcanic clasts (up to 60 cm) and white aphyric pumice clasts. Average grain size: 0.2 - 1 cm.	
	Medium to thick; stratified, reversely to normally graded or	Mostly white pumice (10 mm; up to 15 vol.%) and common white	Explosive

Planar stratified pumice breccia D2-4 **Localities: G, H**	massive; laminated at top. Gradational basal contact with D2-3. Multiple parallel laminations occur in the top 10 cm of each of the two beds.	aphyric pumice (platy shape, imbricated towards SW, up to 3 cm; up to 35 vol.%), crystal fragment, grey andesite, hydrothermally altered volcanic clasts. Average grain size: 0.2 - 80 cm; max. 5 cm.	eruption-fed
Fine pumice breccia D2-5 **Localities: G, H**	Very thick (<3 m), diffusely stratified, overall reversely graded bed. Sharp and conformable basal contacts. Diffuse lenses of coarse (up to 45 cm) white pumice clasts are common.	Mostly angular white pumice (>80 vol.%, mostly <2 mm; max 5 cm) and crystal fragment; minor grey andesite (>10 vol.%, up to 1 cm). Rare out-sized grey andesite clasts (<1 vol.%; 6–40 cm) and hydrothermally altered volcanic clasts (<1 vol.%) are present. Average grain size: 0.2 - 6 cm; max. 50 cm.	Explosive eruption-fed
Cross-bedded pumice breccia-conglomerate D2-6 and D2-8 Localities: G, H, I, J	Thin to very thick tabular and stratified units; cross-bedding in trough (several m in wavelengths) that can be compound (i.e. internally cross-stratified (McKee and Weir, 1953; Allen, 1963) and show opposite palæo-flow directions (Fig. 1). The basal contacts of both units are sharp and commonly cut across stratification in the beds beneath.	Mostly sub-angular to sub-rounded white pumice (10–60 vol.%; up to 150 cm), sub-dominant grey andesite, hydrothermally altered volcanic clasts and crystal fragment (up to 20 vol.%), minor white aphyric pumice. Average grain size: 0.2 - 3 cm; max. 150 cm.	Resedimented and reworked
Planar bedded pumice breccia D2-7 Localities: G, H, I	Very thin to very thick; planar bedded, tabular to lenticular, massive, or reversely or normally graded. Planar cross beds attesting of traction currents commonly occur, and graded beds can be stratified at their top. Sharp basal contact, some scouring. Strong bimodality occurs in medium to very thick beds at localities H and I, with randomly distributed, very coarse white pumice clasts (up to 1 m) in a diffusely stratified matrix mostly composed of white pumice clasts.	Mostly white pumice (>80 vol.%) and sub-dominant hydrothermally altered volcanic clasts and crystal fragment (up to 20 vol.%), grey andesite (<1 vol.%), white aphyric pumice. Average grain size: 0.2 - 1.6 cm; max. 100 cm.	Explosive eruption-fed
Dogashima 3			
Weakly stratified andesite breccia D3 Localities: C, I, J	Extremely thick and clast supported. Weakly stratified to massive, with disorganised, weakly stratified pumiceous matrix. Minimum volume estimated at $2x10^6$ m^3.	Overall monomictic with coarsely porphyritic andesite; minor white pumice and hydrothermally altered volcanic clasts at base. Average grain size is: 20-50 cm; max. 100 cm.	Resedimentation from effusive eruption

Table 3

Unit	Locality	Long axis orientation (°)		Number of measures	Inferred flow orientation		Syn-deposition al faults
		Primary	*Secondary*		*Clast imbrication*	*Cross beds*	*Dip/Dip direction*
D1-1	**B**	265-285	215	7		E to W	
D1-1	**D**			>20			75/210
D1-3	**D**	235-245	225 & 275	18			
D1-8	**D**			3	E to W	E to W; W to E	
D2-3e	**G-east**	235-245		8			
D2-4	**G-east**	235-245		>10	E to W	E to W	
D2-6	**G-west**			>10		E to W; W to E	
D2-6	**H**	220		3			
D2-8	**G-west**			>10		E to W; W to E	
D2-8	**I**	245-265		6			
D2-8	**I**			>10	E to W		
D2-8	**I**			>10	E to W; W to E		
D2-8	**J**			>10	E to W; W to E		